


Telocyte-Derived Exosomes Provide an Important Source of Wnts That Inhibits Fibrosis and Supports Regeneration and Repair of Endometrium

Cell Transplantation
Volume 32: 1–19
© The Author(s) 2023
Article reuse guidelines:
sagepub.com/journals-permissions
DOI: 10.1177/09636897231212746
journals.sagepub.com/home/cll


Tian-Quan Chen^{1,2}, Xiao-Jiao Wei¹, Hai-Yan Liu², Sheng-Hua Zhan³, and Xiao-Jun Yang¹ 

Abstract

Intrauterine adhesions (IUA) often occurred after common obstetrical and gynecological procedures or infections in women of reproductive age. It was characterized by the formation of endometrial fibrosis and prevention of endometrial regeneration, usually with devastating fertility consequences and poor treatment outcomes so far. Telocytes (TCs), as a novel interstitial cell type, present in female uterus with *in vitro* therapeutic potential in decidualization-defective gynecologic diseases. This study aims to further investigate the role of TC-derived Wnt ligands carried by exosomes (Exo) in reversal of fibrosis and enhancement of regeneration repair in endometrium. IUA cellular and animal models were established from endometrial stromal cells (ESCs) and mice, followed with treatment of TC-conditioned medium (TCM) or TC-derived Exo. In cellular model, fibrosis markers (collagen type I alpha I [COL1A1], fibronectin [FN], and α -smooth muscle actin [α -SMA]), angiogenesis (vascular endothelial growth factor [VEGF]), and pathway protein (β -catenin) were determined by quantitative reverse transcription polymerase chain reaction (qRT-PCR), Western blotting (WB), and immunofluorescence. Results showed that, TCs (either TCM or TC-derived Exo) provide a source of Wnts that inhibit cellular fibrosis, as evidenced by significantly elevated VEGF and β -catenin with decreased fibrotic markers, whereas TCs lost salvage on fibrosis after being blocked with Wnt/ β -catenin inhibitors (XAV939 or ETC-159). Further in mouse model, regeneration repair (endometrial thickness, number of glands, and fibrosis area ratio), fibrosis markers (fibronectin [FN]), mesenchymal–epithelial transition (MET) (E-cadherin, N-cadherin), and angiogenesis (VEGF, microvessel density [MVD]) were studied by hematoxylin–eosin (HE), Masson staining, and immunohistochemistry. Results demonstrated that TC-Exo treatment effectively promotes regeneration repair of endometrium by relieving fibrosis, enhancing MET, and angiogenesis. These results confirmed new evidence for therapeutic perspective of TC-derived Exo in IUAs.

Keywords

intrauterine adhesions (IUAs), telocytes (TCs), endometrial stromal cells (ESCs), fibrosis, exosome (Exo)

Introduction

Intrauterine adhesions (IUAs) are partial or total occlusions of uterine cavity caused by trauma or infection in basal layer of endometrium and irreversible damaged self-repair capacity. IUAs are frequently accompanied by various complications, such as hypomenorrhea, amenorrhea, recurrent miscarriage, or even devastating infertility, either of these will severely impact female reproductive health.^{1–3} Endometrial stromal cells (ESCs) are mainly located in basal layer of endometrium and are of great significance for self-renew or regeneration repair of endometrium after cyclic physiological menstruation, trauma, or infection-induced pathological endometrial damage.^{4,5} Wnt/ β -catenin is a key signaling pathway involved in ESCs decidualization and mesenchymal–epithelial

¹ Department of Obstetrics and Gynecology, The First Affiliated Hospital of Soochow University, Suzhou, China

² Department of Obstetrics and Gynecology, The Affiliated Hospital of Yangzhou University, Yangzhou University, Yangzhou, China

³ Department of Pathology, The First Affiliated Hospital of Soochow University, Suzhou, China

Submitted: February 10, 2023. Revised: September 22, 2023. Accepted: October 23, 2023.

Corresponding Authors:

Sheng-Hua Zhan, Department of Pathology, The First Affiliated Hospital of Soochow University, 188 Shizi Road, Suzhou 215006, Jiangsu Province, China. Email: zhanshenghua@suda.edu.cn

Xiao-Jun Yang, Department of Obstetrics and Gynecology, The First Affiliated Hospital of Soochow University, 188 Shizi Road, Suzhou 215006, Jiangsu Province, China. Email: yang.xiaojun@hotmail.com



transition (MET), both were essential for ESCs maturation and endometrium reparation.^{6–9} Damage in number and function of ESCs, including abnormal Wnt/ β -catenin signal pathway, impaired decidualization, and imbalanced epithelial–mesenchymal transition (EMT)/MET process, are all risk factors in the onset or recurrence of IUAs.^{10–12}

Telocytes (TCs) are a newly discovered type of interstitial cell with multiple proposed functions, including paracrine effects, maintaining proliferation and homeostasis, anti-fibrosis in multiple tissues and organs, and so on.^{13–16} Some of these functions were based on experimental evidence, such as exosomes (Exo) derived from cardiac TCs containing multiple abundant microRNAs (miRNAs), which can decrease cardiac fibrosis, increase angiogenesis, and improve cardiac function in rat model of myocardial infarction.¹⁷ Whereas, other proposed functions were highly speculative, merely based on characteristic ultrastructure, and intercellular junctions, thus need extensive investigations. More recently, TCs was found to provide essential non-epithelial Wnt ligand signals for self-renewal and differentiation of local stem cell (SC) niches, maintaining SC-mediated intestinal mucosal regeneration and repair.^{18,19} Our team previously found that Wnt ligands secreted by isolated uterine TCs have the capacity to activate Wnt/ β -catenin pathway, subsequently enhance decidualization and MET process in ESCs *in vitro*.⁷ This preliminary experimental finding is of high importance and raises future perspective application of TCs in decidualization-defective gynecologic diseases.

Based on known involvement of TCs in intestinal mucosa self-renewal^{18,19} and in ESCs enhancement *in vitro*,⁷ the current central hypothesis is that TCs might be a source of local Wnt signal that was essential to maintain integrity of endometrium and reverse traumatic or inflammation-induced endometrium fibrosis/IUAs. In this study, we aim to investigate anti-fibrosis roles of uterine TCs, to observe regeneration repair both in cellular and mouse models of IUAs. Hopefully, these results will add more evidence for therapeutic potential of TCs in fibrosis of endometrium and trauma of uterus.

Materials and methods

Maintenance of animals

Animal experiments were reviewed and approved by the Ethics Committee of Soochow University (ECSU2019000163). Eight-week-old BALB/c-specific pathogen-free female virgin mice, weighing 20–25 g, were purchased from the Laboratory Animal Center of Soochow University. The animals were raised with chow and fresh water in an animal facility with the same controlled conditions (22°C, 14 h:10 h light/dark cycle).

Isolation and primary culture of uterine ESCs

ESCs were isolated, and cultured, as described previously.^{7,20} The uterine tissues of female BALB/c mice were collected

under aseptic conditions and washed three times with phosphate-buffered saline (PBS) containing 100 U/ml penicillin and 0.1 mg/ml streptomycin (Beyotime, Shanghai, China), then minced into 0.5–1 mm³ pieces. Prepared uterine tissue was digested for 90 min at 4°C in 0.5% trypsin (Beyotime, Shanghai, China). The remaining tissue was incubated in Dulbecco's modified eagle medium (DMEM)/F12 (Hyclone, Logan, UT, USA) supplemented with 0.1% type-II collagenase (Sigma-Aldrich China, Inc., Shanghai, China) at 37°C, and dissociated mechanically using a pipette every 15 min, followed by termination of the digestion reaction after 90 min. Subsequently, the resulting suspension was filtered through 100 μ m and 40 sterile nylon-mesh filters (BD Falcon, Heidelberg, Germany). Following centrifugation at 302 \times g for 5 min at room temperature, the supernatant was discarded, and ESCs were gathered and cultured using DMEM/F12 medium supplemented with 10% fetal bovine serum (FBS; Gibco Life Technologies, Grand Island, NY, USA) in a 10 cm dish (Corning, Glendale, AZ, USA) at 37°C in a humidified incubator with 5% CO₂. The complete medium was replaced every other day until they reached confluence. The third to sixth passages were used for subsequent experiments.

Isolation and primary culture of uterine TCs

The isolation and primary culture of uterine TCs were performed according to our previous procedures.^{7,20–22} The uterine was cut longitudinally, and incubated in 0.1% type-II collagenase in DMEM for 60 min at 37°C. Then, the tissue was placed with the luminal side facing up, and the endometrial layer of the uterus was scraped off using a razor, and then minced into 0.5–1 mm³ pieces. The tissue was incubated in 0.1% type-II collagenase for an additional 60 min. Subsequently, the resulting suspension was filtered through 40 μ m sterile filters. The cells were washed with 10% FBS to stop the enzymatic reaction and then washed in PBS. Cells were cultured using DMEM/F12 medium supplemented with 10% FBS in a 10 cm dish for 2 h. The media containing slowly adhering cells were re-plated into a new dish and maintained in culture. After 48 h of incubation, the medium was replaced with serum-free DMEM/F12 medium and then cultured for an additional 24 h. Supernatants were collected and filtered through a 0.45- μ m filter, referred to as TC-conditioned medium (TCM), stored at –80°C for subsequent experiments.

Development of IUA cell model (transforming growth factor-beta 1-treated ESCs)

Mouse transforming growth factor-beta 1 (TGF- β 1; 0, 5, 10, 15, 20, and 25 ng/ml) (BioLegend, San Diego, USA) was administrated to ESCs for 72 h. The protein expression of fibrosis markers collagen type 1 alpha 1 (COL1A1), fibronectin (FN), and α -smooth muscle actin (α -SMA) was

Table 1. List of Antibodies and Labels for WB, Cell IF, and Tissue IHC.

Antibodies and labels	Dilution	Company
CD34	Cell IF 1:500	Abcam, Cambridge, UK
Vimentin	Cell IF 1:500	Abcam, Cambridge, UK
Cytokeratin	Cell IF 1:500	CST, MA, USA
COL1A1	Cell IF 1:300; WB 1:1,000	CST, MA, USA
FN	Cell IF 1:300; WB 1:2,000; tissue IHC 1:300	Proteintech, Wuhan, China
α -SMA	Cell IF 1:300; WB 1:1,000	CST, MA, USA
β -tubulin	WB 1:1,000	CST, MA, USA
CD63	WB 1:1,000	Abcam, Cambridge, UK
TSG101	WB 1:1,000	Abcam, Cambridge, UK
VEGF	WB 1:1,000; tissue IHC 1:300	Proteintech, Wuhan, China
CD-31	Tissue IHC 1:500	Servicebio, Wuhan, China
N-cadherin	Tissue IHC 1:300	CST, MA, USA
E-cadherin	Tissue IHC 1:300	CST, MA, USA
HRP-conjugated goat anti-rabbit or anti-mouse IgG (H + L)	WB 1:3,000; tissue IHC 1:200	Servicebio, Wuhan, China
Cy3-conjugated goat anti-rabbit or anti-mouse IgG (H + L)	Cell IF 1:300	Servicebio, Wuhan, China
FITC-conjugated goat anti-rabbit or anti-mouse IgG (H+L)	Cell IF 1:100	Servicebio, Wuhan, China

WB: Western blotting; Cell IF: Cell immunofluorescence; IHC: immunohistochemistry; CST: cell signaling technology; COL1A1: collagen type I alpha 1; FN: fibronectin; α -SMA: α -smooth muscle actin; VEGF: vascular endothelial growth factor; HRP: horse radish peroxidase.

detected by Western blotting (WB). Preliminary results showed that the protein expression level was most prominent within ESCs after 15 ng/ml TGF- β 1 exposure.

Then, 15 ng/ml TGF- β 1 was chosen to treat ESCs for 0, 12, 24, 48, and 72 h respectively, with the same WB determination of COL1A1, FN, and α -SMA. The results showed that the combination of 15 ng/ml TGF- β 1 and 48 h can reach the highest expression level of three fibrosis markers within ESCs, and therefore, develop the optimal IUA cell model, rendered for experiments that followed.

Treatment with TCM

To observe the reversal potential of TCM on fibrotic ESCs, the established TGF- β 1-treated ESCs IUA model was seeded in six-well plates at a density of 3×10^5 cells/well and cultured in DMEM/F12 (served as control group: TGF- β 1-ESCs + DMEM/F12) or in TCM (TCM group: TGF- β 1-ESCs + TCM) supplemented with 10% FBS *in vitro*, with non-TGF- β 1-treated regular ESCs cultured in DMEM/F12 served as the blank group (regular ESCs + DMEM/F12). Cells were all maintained in a 5% CO₂ incubator at 37°C and harvested after 48 h, and subsequently, the fibrosis markers were determined by WB and immunofluorescence.

Cell immunofluorescence

To observe the morphology of primary TCs and ESCs, double immunofluorescence staining was performed as described previously^{7,21} Briefly, primary TCs and ESCs were individually seeded at a suitable density on slides. After

being fixed with 4% paraformaldehyde and blocked with 3% bovine serum albumin (BSA). TCs and ESCs were incubated with the first primary antibodies overnight at 4°C. Rabbit anti-vimentin and mouse anti-CD34 antibodies for TCs, rabbit anti-vimentin antibody, and mouse anti-pan cytokeratin for ESCs. After washing three times with PBS, both cells were incubated with fluorescein isothiocyanate (FITC)-conjugated goat anti-rabbit immunoglobulin G (IgG) (H + L) or Cy3-conjugated goat anti-mouse IgG (H + L) as secondary antibodies. Nuclei were stained with 4',6-diamidino-2-phenylindole (DAPI; Servicebio, Wuhan, China). Then, observed and imaged under an inverted fluorescent microscope (Nikon, Tokyo, Japan).

Meanwhile, similar immunofluorescence was also performed to observe fibrosis markers among three groups (blank, control, and TCM groups) as described above. The secondary antibody was Cy3-conjugated goat anti-mouse IgG (H + L) or Cy3-conjugated goat anti-rabbit IgG (H + L). The antibodies and labels were listed in Table 1.

Extraction, determination, and identification of TC-derived Exo

After the effectiveness of reversal on fibrosis was confirmed in TCM, Exo from TCM was extracted for further investigation using exoEasy Maxi Kit (Qiagen, Hilden, Germany) according to manufacturer's instruction. Briefly, TCM was mixed with a binding buffer called XBP buffer in a 1:1 ratio. The buffer media were then loaded into exoEasy spin columns and centrifuged at $500 \times g$ for 1 min. Then, the flow-through was discarded, followed with 10 ml washing buffer

named XWP buffer added into each column and centrifuged at $5,000 \times g$ for 5 min to remove residual buffer; 400 μ l of elution buffer called XE buffer was added to the membrane of the columns and incubated for 1 min, followed with centrifugation at $500 \times g$ for 5 min. Then, re-apply the eluate to the exoEasy spin column membrane and incubate for 1 min and centrifuge at $5,000 \times g$ for 5 min to collect the eluate. The Exo was collected in eluate and stored at -80°C for subsequent cell and animal model studies.

Protein contents in Exo were determined for the subsequent quantification of WB experiments and administration dosage using PierceTM BCA Protein Assay Kit (Thermo Scientific, USA) according to the instruction manual. Briefly, Exo sample mixed with BCA working solution was incubated at 37°C for 30 min, then optical density (OD) value was tested at the wavelength of 562 nm. Size and concentration of Exo particles were determined using nanoparticle tracking analysis (NTA) with ZetaView PMX 110 (ZetaView software edition 8.04.02, Particle Metrix, Meerbusch, Germany). Briefly, as described previously,^{23,24} isolated Exo samples were appropriately diluted using PBS buffer (Biological Industries, Israel), and NTA measurement was analyzed and recorded at 11 positions. The ZetaView system was calibrated using 110 nm polystyrene particles. The temperature was maintained at around 28°C .

The morphology of Exo was observed under transmission electron microscope (TEM). A 20 μ l suspension with Exo was negatively stained by phosphotungstic acid and fixed on copper mesh for 10 min at room temperature.^{25,26} The mesh was thoroughly dried before viewing and then observed under a TEM (JEOL, JEM-1200EX, Japan).

Meanwhile, WB was used to examine expression of CD63 and TSG101 in three independent samples, both markers are specific surface proteins pertaining to Exo.^{27,28}

Vascular endothelial growth factor production in ESCs

Vascular endothelial growth factor (VEGF) is a specific substance for angiogenesis within endometrium which is produced by ESCs and is relevant to cyclic menstruation and endometrial regeneration.²⁹ TC-derived Exo was separately added into culture medium of TGF- β 1-treated ESCs (3×10^5 cells/well) with a final concentration of 5 $\mu\text{g}/\text{ml}$, served as TC-Exo group (TGF- β 1-ESCs + TC-Exo). Meanwhile, TGF- β 1-treated and non-TGF- β 1-treated regular ESCs served as control (TGF- β 1-ESCs) and blank group (regular ESCs). After 48-h incubation, VEGF in three groups (blank, control, and TC-Exo group) was determined by quantitative real-time polymerase chain reaction (qRT-PCR) for mRNA and WB for protein in ESCs. And total VEGF in the culture medium released from ESCs was measured by a mouse VEGF Quantikine ELISA kit (R&D Systems, MN, USA) according to manufacturer's instructions. The absorbance of

samples was read at 450 nm using a microplate reader (BioTek Instruments Inc., USA).

Role of Wnt ligands and Wnt/ β -catenin pathway

To investigate whether the observed *in vitro* anti-fibrosis effect results from Wnt ligands carried by TC-derived Exo ETC-159 (MCE, Shanghai, China), a small molecule inhibitor of porcupine (PORCN) which provides essential palmitoylation for secretion of active Wnt proteins was used to block Wnt ligand production within TCs.^{30–32} A final concentration of 100 nM ETC-159 diluted by serum-free DMEM/F12 medium was co-cultured with TCs for 24 h. The supernatant was collected and used for Exo extraction (ETC-159 treated TC-derived Exo) as mentioned above. Then, both Exo (TC-derived Exo and ETC-159-treated TC-derived Exo) were separately added into the culture medium of TGF- β 1-treated ESCs (3×10^5 cells/well) with a final concentration of 5 $\mu\text{g}/\text{ml}$, served as TC-Exo (TGF- β 1-ESCs + TC-Exo) and ETC-TC-Exo (TGF- β 1-ESCs + ETC-159-TC-Exo) group, respectively. Meanwhile, TGF- β 1-treated and non-TGF- β 1-treated regular ESCs cultured in DMEM/F12 served as control (TGF- β 1-ESCs) and blank (regular ESCs) groups, respectively, as mentioned earlier. Four groups of ESCs were incubated in the same conditions for 48 h, then harvested for WB determination of fibrosis markers (COL1A1, FN, and α -SMA), and pathway protein β -catenin.

Meanwhile, to observe involvement of Wnt pathway in reversal of fibrotic ESCs, XAV939 (MCE, Shanghai, China), a small molecule inhibitor of Wnt/ β -catenin pathway, which is capable of blocking Wnt signaling through upregulating degradation of β -catenin by stabilizing the axin protein, was used to inhibit Wnt/ β -catenin signaling pathway within ESCs.^{33,34} A final concentration of 1 μM XAV939 was applied to reaction system containing TGF- β 1-treated ESCs and TC-derived Exo with a final concentration of 5 $\mu\text{g}/\text{ml}$, served as TC-Exo + XAV939 group (TGF- β 1-ESCs + TC-Exo + XAV939). Group settings (blank, control, and TC-Exo group) and procedures were the same as above-mentioned. Four groups of ESCs were incubated in the same conditions for 48 h, and fibrosis markers (COL1A1, FN, and α -SMA) and pathway protein (β -catenin) were determined with WB.

Quantitative real-time polymerase chain reaction

To measure mRNA expression of fibrosis marker COL1A1, FN, and α -SMA (Acta2), total RNA was lysed and extracted using TRIzol reagent (Invitrogen, Carlsbad, CA, USA) according to manufacturer's instructions. The concentration and purity of the RNA were determined using a UV spectrophotometer (260 nm, Thermo Scientific, MA, USA). Briefly, 1 μg of cellular RNA was reverse transcribed into cDNA using a PrimeScriptTM RT Master Mix kit (Takara, Kyoto, Japan) to a final volume of 10 μl . Then, 1 μl of cDNA was

Table 2. List of qRT-PCR Primers.

Gene	Forward	Reverse
COL1A1	GCTCCTCTTAGGGGCACT	CCACGTCTCACCATTGGGG
FN	ATGTGGACCCCTCCTGATAGT	GCCCAGTGATTTCAGCAAAGG
α -SMA	GTCCCAGACATCAGGGAGTAA	TCGGATACTTCAGCGTCAGGA
GAPDH	AGGTCGGTGTGAACGGATTG	TGTAGACCATGTAGTTGAGGTCA

qRT-PCR: quantitative real-time polymerase chain reaction; COL1A1: collagen type I alpha 1; FN: fibronectin; α -SMA: α -smooth muscle actin.

added into PowerUpTM SYBRTM Green Master Mix (Thermo Scientific, Waltham, MA, USA) to a final volume of 20 μ l. Amplification was performed on an ABI QuantStudio3 Detection System (Applied Biosystems, Carlsbad, CA, USA). The $2^{-\Delta\Delta C_t}$ method was used to determine the relative quantification in each sample. All reactions were triple duplicated under the same conditions. The house-keeping gene GAPDH (glyceraldehyde-3-phosphate dehydrogenase) was used as an internal reference gene to normalize individual samples. The primer sequences are provided in Table 2.

Western blotting

WB was performed as previously described^{7,21} to measure the protein expression. Briefly, total proteins were extracted using RIPA (radioimmunoprecipitation assay) lysis buffer (Beyotime, Shanghai, China) containing a protease inhibitor cocktail (BBI, Shanghai, China). After determining the concentration using a PierceTM BCA Protein Assay Kit (Thermo Scientific, USA), the proteins were resolved by 5%–12% sodium dodecyl-sulfate (SDS)-polyacrylamide gel, and then electrotransferred to 0.45 μ m polyvinylidene fluoride (PVDF) membrane (Millipore, Billerica, MA, USA), followed by immunoblotting with the corresponding primary antibodies. Labeled with secondary antibodies, then, detected with an enhanced chemiluminescence kit (Absin Bioscience Inc., Shanghai, China). Results were photographed using a gel imaging system (Tanon, Shanghai, China) and analyzed by ImageJ software (ImageJ 1.53k, NIH). The expression levels of individual proteins were expressed as a ratio relative to the internal reference protein expression of β -tubulin. The antibodies and labels were listed in Table 1.

IUA mouse model

The mouse model of endometrial fibrosis or IUAs was established by the combination of mechanical uterine curettage and inflammatory lipopolysaccharides (LPSs) injection into uterine cavity as described in the literature.^{35,36} Briefly, daily vaginal smears proved estrum mice were anesthetized with an intraperitoneal injection of 1.25% avertin. Through vertical dorsal incision, the uterus was exposed, and uterine horn was mechanically injured with a rough surface needle inserted through the lumen and

scratched up and down 50 times until the uterine inner wall became rough. A single dose of 20 μ l LPS (10 mg/ml; Beyotime, Shanghai, China) was then injected into the uterine cavity to induce inflammatory damage, with both ends of the punctuation site sealed by tweezers for 5 min to avoid any liquid leakage. A pseudo-operation that received only vertical dorsal incision without any mechanical and inflammation intervention on uterine tissues served as sham control. After surgery, the mice received a prophylactic intramuscular injection of a single dose of 20,000 U penicillin (Solarbio, Beijing, China). Then, 5 days later, six mice were randomly assigned at 1:1 ratio into two groups, with three in each group: (A) IUA-TC-Exo group, (B) IUA group. Together with three in pseudo-operation served as the sham group (C).

Briefly, groups A and B received three doses of intrauterine injections (5 days apart) through the original incision with TC-derived Exo (200 μ g/ml) for group A and 20 μ l PBS for group B, with both ends of the punctuation site sealed by tweezers for 5 min to prevent any liquid leakage. The mice were maintained with the same procedure after each injection. Then, after the third injection, mice in all groups were sacrificed and uterine tissues were collected at the estrum.

Hematoxylin–eosin, Masson staining, and immunohistochemistry staining

Mouse uterine samples were fixed in 4% paraformaldehyde, embedded in paraffin, and sectioned at 5 mm. Hematoxylin–eosin (HE) and Masson trichrome staining were performed to observe endometrial histopathology and collagen content to evaluate IUA, respectively. Masson trichrome staining was performed using a Masson staining kit (Servicebio, Wuhan, China). For results evaluation, endometrial thickness measurements were obtained from the lateral sides of each cross-section under high-magnification fields. Briefly, a total of eight high-power fields (HPFs) ($\times 400$) with 45° intervals in each cross-section were chosen, measured, and averaged for each HE-stained section. Similarly, the glands numbers in three HPF ($\times 400$) were randomly selected, counted, and averaged to determine endometrial gland abundance. On the other hand, the fibrosis area ratio was calculated as follows: total area of endometrial fibrosis per field/ the sum area of endometrial stroma and gland in Masson stained slice.³⁷ Images were analyzed using the ImageJ software (ImageJ 1.53k, NIH, USA).

For immunohistochemistry (IHC) staining, the slides were dewaxed and rehydrated, endogenous peroxidase activity was blocked with 3% hydrogen peroxide. Then, after blocking with 3% BSA for 1 h at room temperature, the slides were incubated at 4°C overnight with primary antibodies, including FN, E-cadherin, N-cadherin, VEGF, CD-31 (Table 1). FN is a fibrosis maker, E-cadherin and N-cadherin are closely related to EMT/MET phenotype. VEGF and CD31 were performed to assess angiogenesis and microvessel density (MVD). After being washed with PBS (PH = 7.4), slices were incubated with horse radish peroxidase (HRP)-conjugated goat anti-mouse/rabbit IgG (Table 1) as the secondary antibody for 50 min at room temperature. Then, DAB Substrate System (Servicebio, Wuhan, China) was used to reveal the IHC staining. Images were captured by an inverted microscope (CIC XSP-C204, China).

Results of immunostaining (FN, E-cadherin, N-cadherin, VEGF) were evaluated using IHC score,³⁸ which was calculated by multiplying the staining intensity score and percentage score. The staining intensity was divided into four scores: 0 (negative, no staining), 1 (weak, light brown), 2 (medium, brown), and 3 (strong, dark brown). Scores were combined to generate each IHC score (min, 0; max, 4). The analysis was performed by ImageJ software (ImageJ 1.53k, NIH, USA).

MVD was recorded as the number of CD31-positive endothelial cells or endothelial cell clusters per HPF ($\times 400$) from at least four areas with the highest vascularization.³⁹

Statistical analysis

Statistical analysis was performed using GraphPad Prism 8 (GraphPad Software, La Jolla, CA, USA). Data are expressed as mean \pm standard deviation (SD). One-way analysis of variance (ANOVA) was used to evaluate differences between three or multiple groups, followed with Tukey's test for post hoc pairwise comparisons. The Shapiro–Wilk test was implemented to validate normal distribution. Statistical significance was set at $P < 0.05$.

Results

Morphological and immunophenotype of ESCs and TCs

Primary ESCs show typical fusiform morphology with clear outline, sparse intercellular links, and vimentin (+)/cytokeratin (–) immunofluorescence staining (Fig. 1A), consistent with our previous results.⁷

Primary uterine TCs show irregular or spindle cellular body with long and characteristic telopodes (Tps), which displayed alternating thin podomers and thick podoms segments. TCs show a typical immunophenotype of double-positive vimentin/CD34, with green and red immunofluorescence staining overlapping each other along the whole length of the cellular body and Tps (Fig. 1B, C).

Successful development of IUA cell model (TGF- β 1-induced ESCs)

To induce cell fibrosis, primary ESCs were exposed to TGF- β 1 with a combination of different concentrations and treatment times. WB results showed fibrosis markers (COL1A1, FN, and α -SMA) were in a concentration-dependent and time-dependent manner. For different concentrations, 15 ng/ml TGF- β 1 can yield peak values of three markers (ANOVA, all P values < 0.05), with no significant elevation compared with 20 ng/ml (ANOVA, post hoc paired test, P value > 0.05) (Fig. 2A). Then, 15 ng/ml TGF- β 1 was chosen to determine the optimal treatment time, which can yield peak values of three markers (ANOVA, all P values < 0.05) at 48 h, with no significant elevation compared with 72 h (ANOVA, post hoc test, P value > 0.05) (Fig. 2B). Therefore, the combination of 15 ng/ml TGF- β 1 with 48 h is the most effective to induce cell fibrosis and develop IUA cell model.

TCM reversed fibrosis in IUA cell model

The reversal effect of TCM on TGF- β 1-induced ESCs fibrosis was evidenced by qRT-PCR and WB determination of fibrosis markers (COL1A1, FN, and α -SMA). Results showed that when exposed to TCM, mRNA and protein expression decreased significantly in TGF- β 1-induced ESCs than in control group (ANOVA, post hoc paired test, all P s < 0.05), suggesting exact reversal effect of fibrosis. Together with a significant decrease between control and blank ($P < 0.05$), adding evidence of successful development of IUA cell model (Fig. 3A, B). Meanwhile, the decreased expression of COL1A1, FN, and α -SMA was also confirmed by immunofluorescence staining (Fig. 3C). Thus, confirmed the exact anti-fibrosis effect in IUA cell model by TCs.

Identification of TC-derived Exo

The morphology of Exo was observed under TEM. Exo was elliptical or round vesicles with intact capsules and uneven sizes (Fig. 4A). The mean diameter of particle measured by NTA was 159.4 ± 54.9 nm, which was confirmed by TEM as well. The original concentration of Exo was 3.5×10^9 particles/ml, with peak distribution when particle size was 138.6 nm (Fig. 4B). This was within the size of extracellular vesicles ranging from 45 nm to 1 μ m reported before.⁴⁰ Meanwhile, WB analysis confirmed expression of CD63 and TSG101 (Fig. 4C), which were specific surface proteins and expected to be presented in Exo.^{27,28}

TC-derived Exo reversed fibrosis and enhanced VEGF secretion in IUA cell model

Reversal of fibrosis by TC-derived Exo in IUA cell model was evidenced by WB determination of fibrosis markers (COL1A1, FN, and α -SMA). Results showed that protein expression increased in the control group (TGF- β 1-ESCs)

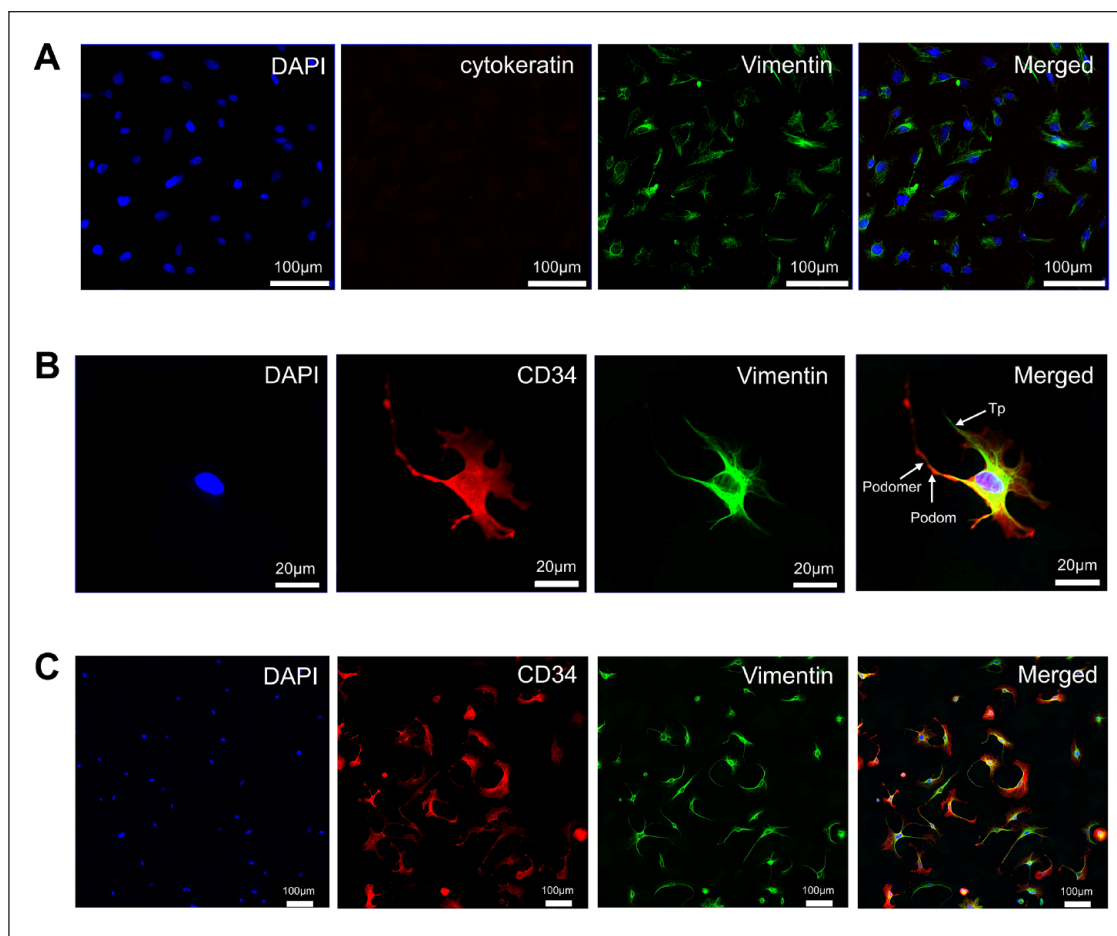


Figure 1. Morphology and immunophenotype of mouse uterine ESCs and TCs observed by immunofluorescence staining and inverted fluorescent microscope. Nuclei were counterstained with DAPI (blue). (A) Immunofluorescence staining of ESCs was positive for Vimentin (green) and negative for cytokeratin. Scale bar = 100 μ m. (B) TCs were typical mesenchymal cells with a characteristic oval cellular body and long extensions named telopodes (Tps), composed of alternating thin (podomer) and thick (podom) segments under high-magnification fields. Double positive for Vimentin (green) and CD34 (red). In the merged image, both immunofluorescence signals overlapped each other along entire cellular body and Tps, with the podomer, and podom indicated. Scale bar = 20 μ m. (C) Immunofluorescence staining of TCs was positive for Vimentin (green) and CD34 (red) under low-magnification fields. Scale bar = 100 μ m. ESC: endometrial stromal cell; TC: telocyte; DAPI: 4'6-diamidino-2-phenylindole.

than in blank (regular ESCs), but decreased significantly in the TC-Exo group (TGF- β 1-ESCs + TC-Exo) (ANOVA, post hoc paired test, all P s < 0.05) (Fig. 5A). Thus, confirmed the salvage or anti-fibrosis effect in IUA cell model by TC-derived Exo.

VEGF in groups of ESCs was determined by qRT-PCR for mRNA, WB for protein, and ELISA for culture media, respectively. Results showed VEGF mRNA and protein expression in the control group (TGF- β 1-ESCs) decreased significantly than in blank (regular ESCs) but elevated significantly after TC-derived Exo salvage in TC-Exo group (TGF- β 1-ESCs + TC-Exo) (ANOVA, post hoc paired test, all P < 0.05) (Fig. 5B, D). Meanwhile, media VEGF determined by ELISA showed statistical differences among groups, with the highest in TC-Exo group (ANOVA, all P < 0.05) (Fig. 5C). Thus, indicated the fibrosis TGF- β 1-ESCs

and weakened VEGF production was relieved or reversed after TC-derived Exo exposure.

Role of Wnt ligands and Wnt/ β -catenin pathway

Involvement of Wnt/ β -catenin in reversal of fibrotic ESCs was proved either in TCs blocked by ETC-159 or in ESCs blocked by XAV939, with the previous one aimed to block production of Wnt ligands, and the later one function to block Wnt/ β -catenin pathway.

For ETC-159 experiment, TCs were pre-treated with ETC-159 and followed with Exo collection from cultural medium, named as ETC-159 treated TC-derived Exo (ETC-TC-Exo), together with the collection of regular TC-derived Exo. Four groups were designed: blank group (regular ESCs), control group (TGF- β 1-ESCs), TC-Exo group

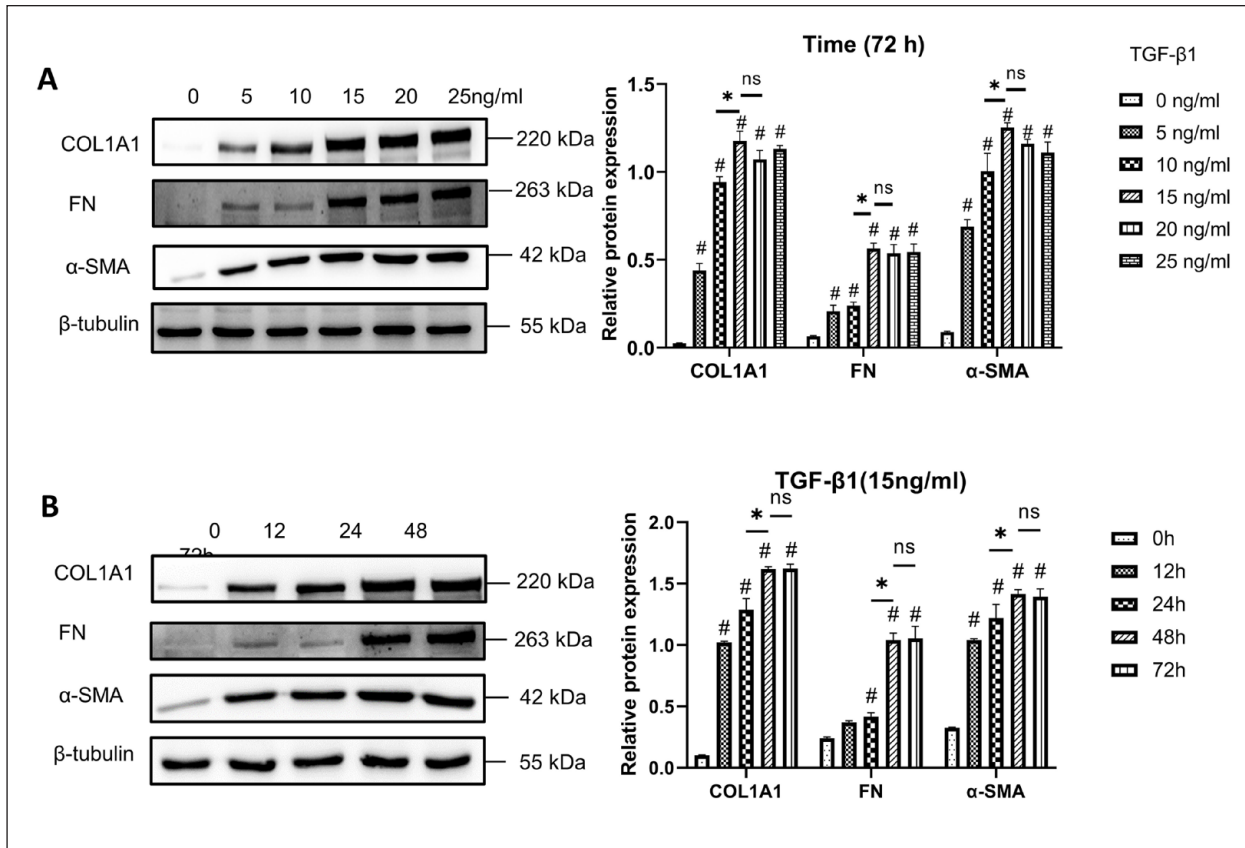


Figure 2. Time and dose-dependent effects of TGF-β1 on fibrosis markers expression (COL1A1, FN, and α-SMA) in regular ESCs analyzed by WB. β-Tubulin served as loading control for WB. Error bars indicated standard deviation (SD) from three independent experiments (biological replicates). $^{\#}P < 0.05$ compared with the control group (0 ng/ml or 0 h). $^{*}P < 0.05$, by one-way ANOVA with Tukey's post hoc test, whereas ns indicates non-significant. (A) WB analysis showed that three markers in regular ESCs reach peak value at 15 ng/ml TGF-β1, with no statistical difference at 20 ng/ml. (B) 15 ng/ml TGF-β1 can yield peak value for three markers at 48 h, with no statistical difference at 72 h. COL1A1: collagen type I alpha I; FN: fibronectin; α-SMA: α-smooth muscle actin; ESC: endometrial stromal cell; WB: Western blotting; ANOVA: analysis of variance; TGF-β1: transforming growth factor-beta 1.

(TGF-β1-ESCs + TC-Exo), and ETC-TC-Exo group (TGF-β1-ESCs + ETC-TC-Exo). Results showed that ETC-TC-Exo experienced a significant loss of fibrosis reversal when compared with regular TC-derived Exo (ANOVA, post hoc paired test, all $P_s < 0.05$) (Fig. 6A). This suggested that TCs lose their salvage effect on fibrosis when conditionally depleted in the Wnt ligands which were contained within its Exo.

For XAV939 experiment, four groups were designed: blank group (regular ESCs), control group (TGF-β1-ESCs), TC-Exo group (TGF-β1-ESCs + TC-Exo), and TC-Exo + XAV939 group (TGF-β1-ESCs + TC-Exo + XAV939). ESCs samples from all groups were collected for WB determination of fibrosis markers and β-catenin. Results showed that β-catenin increased in TC-Exo group (ANOVA, post hoc paired test, all $P_s < 0.05$), together with significantly decreased fibrosis markers (ANOVA, post hoc paired test, all $P_s < 0.05$). However, TC-derived Exo lost its salvage on

fibrosis in TGF-β1 treated ESCs blocked by XAV939 in the TC-Exo + XAV939 group, manifested as opposite trends of these markers (ANOVA, post hoc paired test, all $P_s < 0.05$) (Fig. 6B).

Morphometric analyses of endometrial thickness, glands, and fibrosis

Morphometric analyses indicated a successfully established IUA mouse model and the exact reversal effect on fibrosis by TC-Exo. First, histopathology observation (Fig. 7A) showed markedly decreased endometrium thickness and density of glands in IUA model group. These were totally different from the normal and intact endometrial structure in the Sham group, which have glandular epithelial cells, glands duct and capillaries fully developed. As shown in Fig. 7A, endometrial thicknesses were 519.80 ± 15.20 , 384.70 ± 21.58 , and $440.70 \pm 18.84 \mu\text{m}$, with endometrial

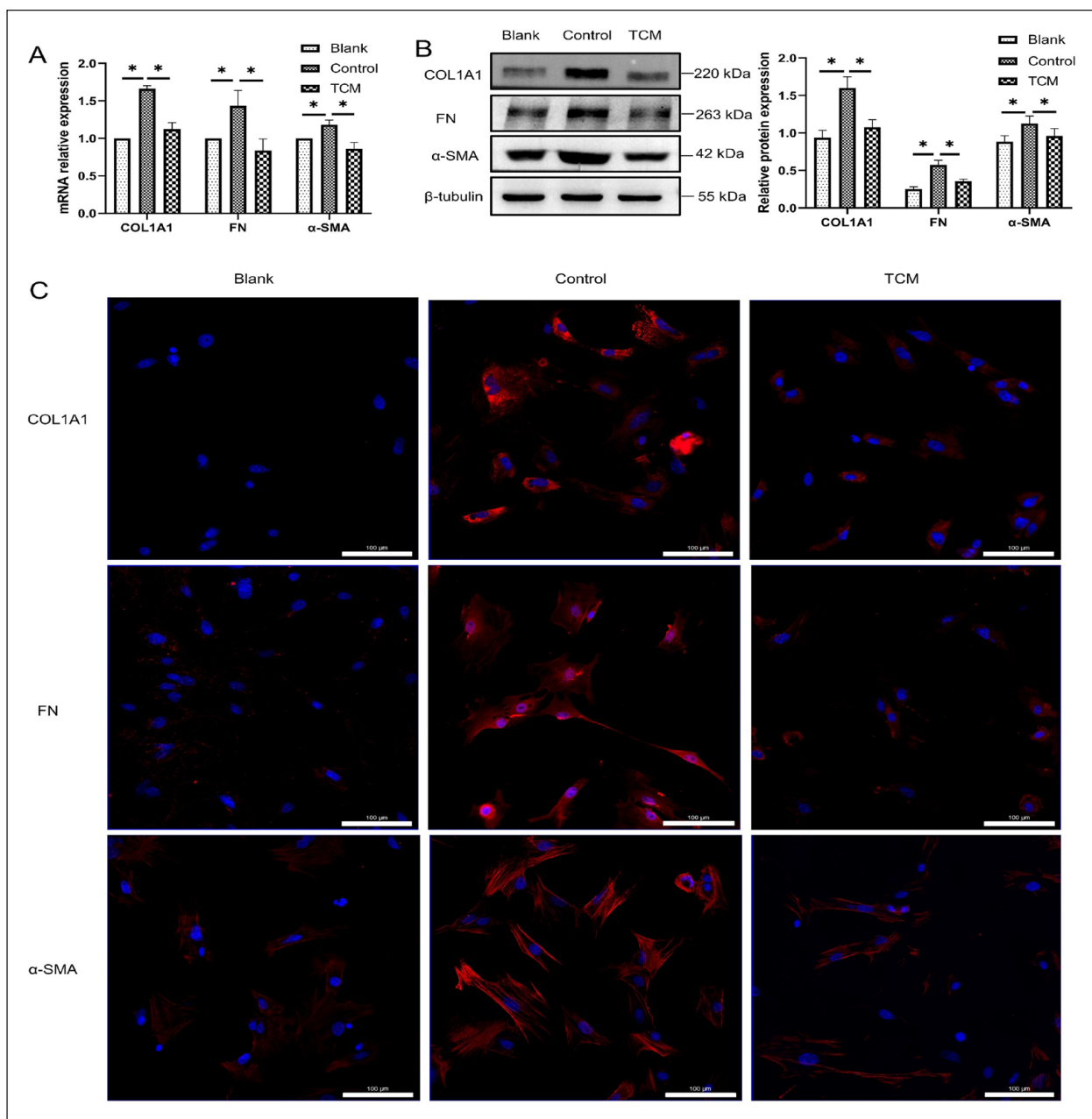


Figure 3. TCM exposure reversed and downregulated fibrosis markers (COL1A1, FN, and α-SMA) in TGF-β1-treated ESCs. Error bars indicated SD from three independent experiments (biological replicates). * $P < 0.05$, by one-way ANOVA with Tukey's post hoc test. mRNA (A) and protein (B) expression decreased significantly in TCM group (TGF-β1-ESCs + TCM), as compared with control (TGF-β1-ESCs + DMEM/F12) and blank cells (regular ESCs + DMEM/F12). Relative mRNA expression was determined by normalizing to GAPDH levels for qRT-PCR. β-tubulin served as loading control for WB. (C) Immunofluorescence staining demonstrated the down-expression of three proteins. Scale bar = 100 μm. TCM: TC-conditioned medium; COL1A1: collagen type I alpha I; FN: fibronectin; α-SMA: α-smooth muscle actin; ESC: endometrial stromal cell; SD: standard deviation; WB: Western blotting; ANOVA: analysis of variance; mRNA: messenger RNA; qRT-PCR: quantitative real-time polymerase chain reaction; TGF-β1: transforming growth factor-beta I; DMEM: Dulbecco's modified eagle medium.

glands numbers being 14.330 ± 3.283 , 6.667 ± 0.333 , and 8.889 ± 1.711 per HPF in the sham, IUA, and IUA-Exo groups, respectively. When compared with the sham group, a statistically thinner endometrium and a lesser number of glands were observed in IUA group (ANOVA, post hoc

paired test, all $P_s < 0.05$). Whereas endometrium thickness was significantly salvaged by TC-derived Exo treatment (ANOVA, post hoc paired test, all $P_s < 0.05$), and the number of glands in the IUA-Exo group was higher than in the IUA group but the difference was no statistically significant

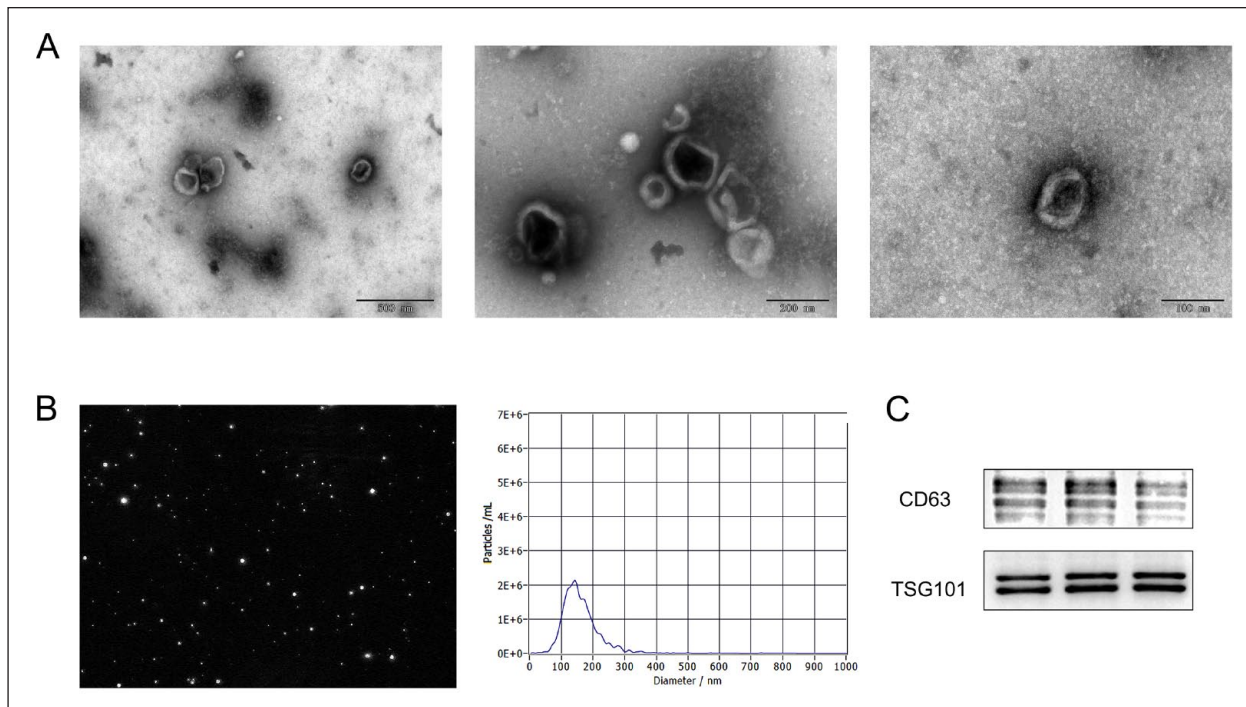


Figure 4. Identification and characterization of TC-derived Exo. (A) Transmission electron micrographs of exosomes. Scale bar (from left to right): 500, 200, 100 nm, respectively. (B) NTA of TC-derived exosomes. Relationship between mean diameter (159.4 ± 54.9 nm) and original concentration of Exo (3.5×10^9 particles/ml), with peak distribution when particle size being 138.6 nm. (C) WB was used to identify the expression of CD63 and TSG101, both were specific surface proteins pertaining to Exo. Lanes 1, 2, and 3 represent three repeats. TC: telocyte; NTA: nanoparticle tracking analysis; WB: Western blotting.

(ANOVA, post hoc paired test, $P > 0.05$) (Fig. 7C). Thus, provide evidence that endometrium damage can be partially rescued by TC-derived Exo treatment.

Then, quantitative analysis showed TC-derived Exo treatment obviously decrease fibrosis area of the endometrium (ANOVA, all P s < 0.05). Masson staining demonstrates blue collagen fibers and red in mucosa, submucosa, muscles, and blood vessels (Fig. 7B). Results demonstrated that IUA group showed a significantly increased ratio of fibrotic areas ($64.27 \pm 4.36\%$) compared with the sham group ($19.93 \pm 10.37\%$), whereas, TC-Exo treatment can yield a significantly reduced ratio to $30.72 \pm 5.40\%$ (ANOVA, post hoc paired test, $P < 0.05$) (Fig. 7C).

Finally, as we know, FN constitutes a key component in extracellular matrix (ECM) and plays important role in the process of endometrium fibrosis.⁴¹ IHC results demonstrated a significant difference of FN in endometrium among three groups (ANOVA, all P s < 0.05) (Fig. 8), with the highest IHC score in IUA group (1.716 ± 0.08153) compared with the sham group (1.291 ± 0.08062) (ANOVA, post hoc paired test, $P < 0.05$). Whereas, TC-Exo treatment can significantly reduce IHC score to 1.521 ± 0.03281 (ANOVA, post hoc paired test, $P < 0.05$). In other words,

TC-Exo can reduce FN expression in IUA endometrium. This is consistent with the reduced fibrosis areas detected by Masson staining.

TC-derived Exo enhanced angiogenesis in IUA model

MVD, an indicator of angiogenesis, was evaluated by immunostaining quantification of endothelial marker CD31. Results showed that neovascularization in IUA group (31.50 ± 2.136) significantly decreased compared with the sham group (54.33 ± 8.032), whereas TC-Exo treatment significantly increased CD31 immunostaining (47.33 ± 3.538) (ANOVA, all P s < 0.05). This result indicated an obvious angiogenic effect of TC-derived Exo (Fig. 8).

Meanwhile, VEGF, a pro-angiogenic marker, was analyzed by IHC. The IHC score was 1.304 ± 0.1672 , 1.183 ± 0.09087 , and 1.304 ± 0.1833 in the sham, IUA, and IUA-Exo groups, respectively. Semi-quantitative analysis showed a similar trend as MVD, but lack of statistical difference among three groups (ANOVA, all P s > 0.05) (Fig. 8). This suggested that, in addition to the VEGF pathway, multiple factors engaged in TC-derived angiogenic activities.

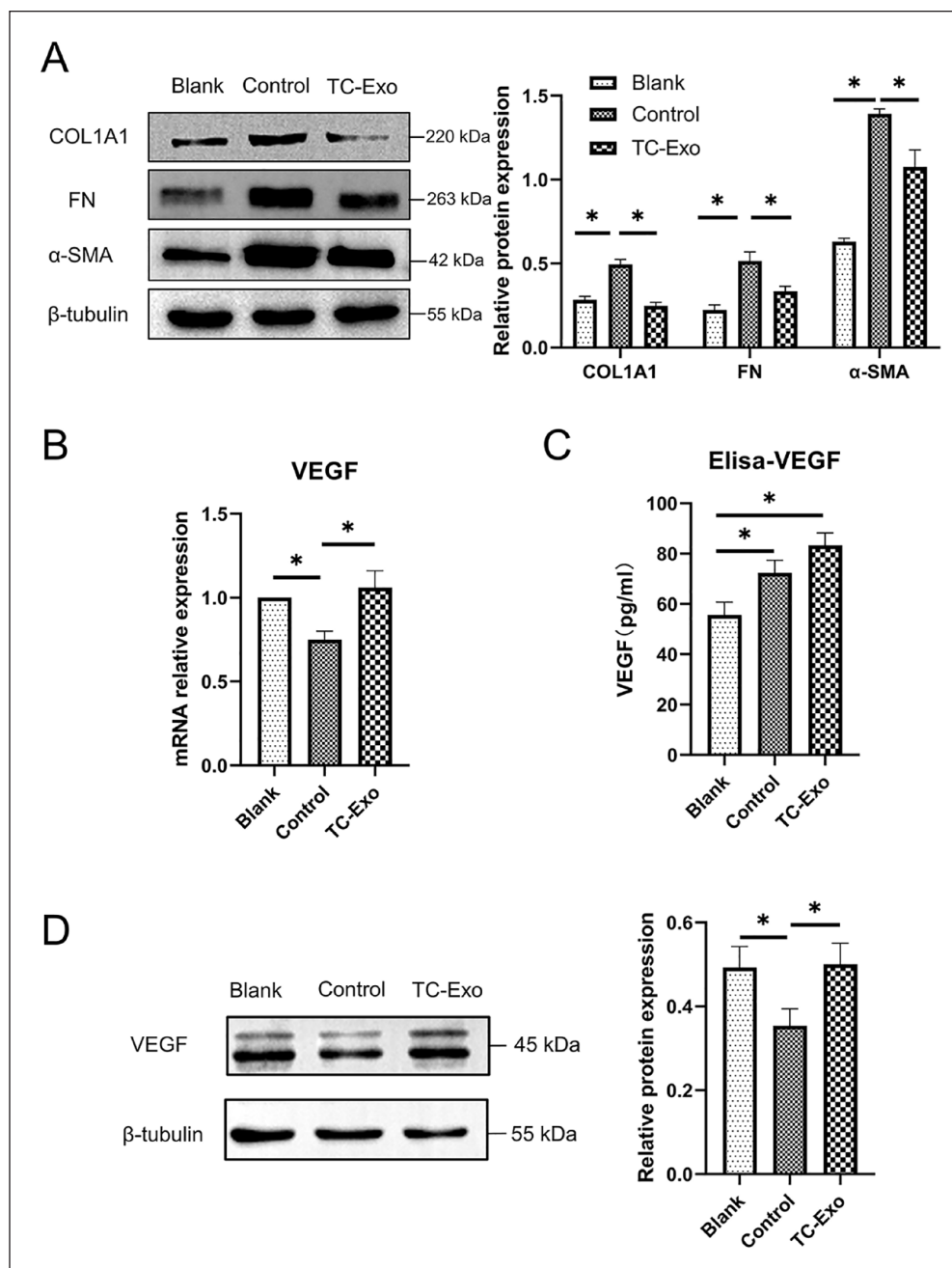


Figure 5. Reversal of fibrosis and enhanced secretion of VEGF in TGF- β 1-treated ESCs when exposed to TC-derived Exo. Error bars indicate SD from three independent experiments (biological replicates). * $P < 0.05$, by one-way ANOVA with Tukey's post hoc test. (A) WB analysis demonstrated that TC-derived Exo treatment significantly decreased fibrosis markers (COL1A1, FN, and α -SMA) in TGF- β 1-induced ESCs among three groups (blank group: regular ESCs; control group: TGF- β 1-ESCs; TC-Exo group: TGF- β 1-ESCs + TC-Exo). β -Tubulin served as loading control. VEGF mRNA (B) and protein (D) expression in control ESCs (TGF- β 1-ESCs) decreased significantly than in blank control (regular ESCs), with significant elevation after TC-derived Exo exposure (TGF- β 1-ESCs + TC-Exo). Relative mRNA expression was determined by normalizing to GAPDH levels for qRT-PCR and β -tubulin served as loading control for WB. (C) Total amount of VEGF in culture media showed statistical difference among three groups, with the highest in TC-Exo group. VEGF: vascular endothelial growth factor; ESC: endometrial stromal cell; TC: telocyte; SD: standard deviation; ANOVA: analysis of variance; WB: Western blotting; COL1A1: collagen type I alpha I; FN: fibronectin; α -SMA: α -smooth muscle actin; mRNA: messenger RNA; TGF- β 1: transforming growth factor-beta 1.

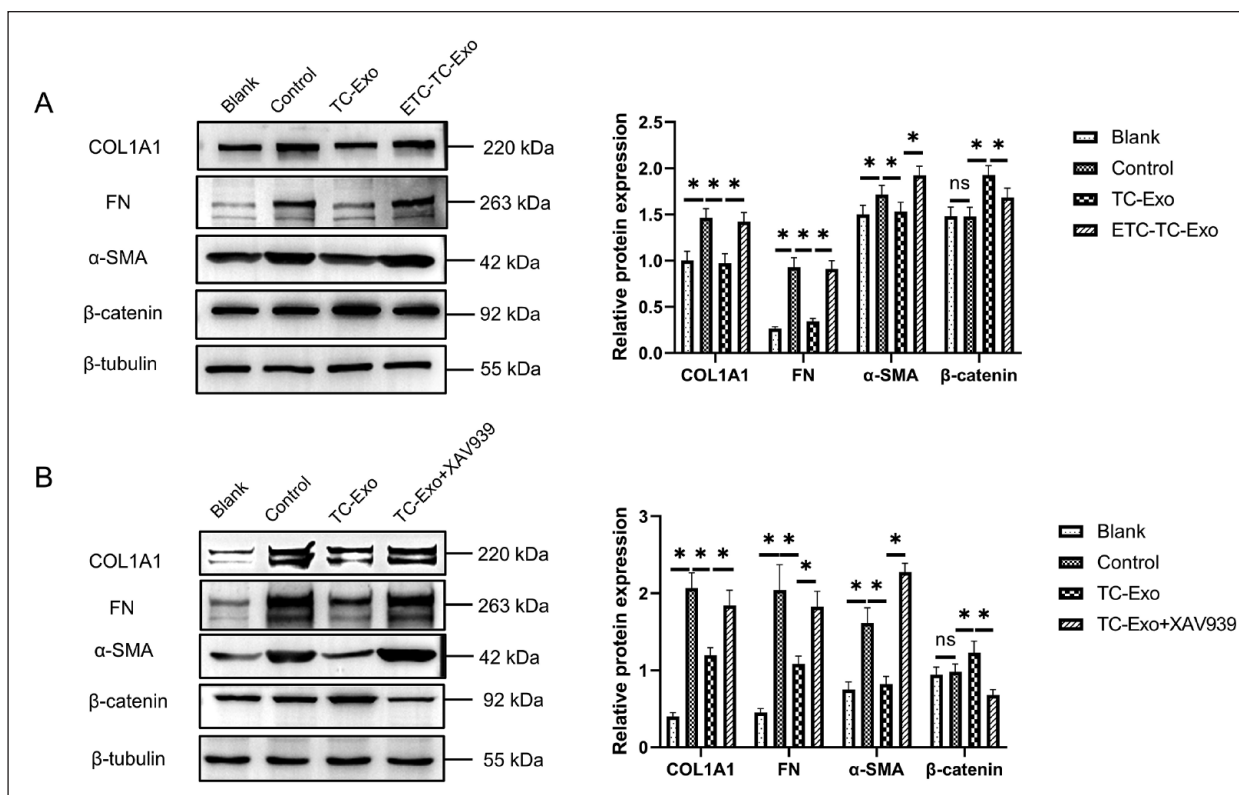


Figure 6. Reversal of fibrosis in TGF- β 1-treated ESCs was antagonized by ETC-159 or XAV939 through blocking of Wnt ligands in TCs or Wnt/ β -catenin pathway in ESCs. β -tubulin served as loading control. Error bars indicated SD from three independent experiments (biological replicates). * $P < 0.05$ by ANOVA with Tukey's post hoc test, whereas ns indicates non-significant. WB analysis detected significant increase of β -catenin, with decreased fibrosis markers (COL1A1, FN, and α -SMA protein) in TGF- β 1-treated ESCs exposed to TC-derived Exo. Whereas, ETC-159 (A) and XAV939 (B) treatment blocked the salvage of TC-derived Exo on fibrosis, with opposite trends of these markers. ESC: endometrial stromal cell; TC: telocyte; SD: standard deviation; ANOVA: analysis of variance; WB: Western blotting; COL1A1: collagen type I alpha I; FN: fibronectin; α -SMA: α -smooth muscle actin; TGF- β 1: transforming growth factor-beta 1.

TC-derived Exo enhanced E-cadherin

E-cadherin, an epithelial adhesion molecule, is functionally linked to generation and maintaining of polarized epithelial phenotype and regulating tissue homeostasis.^{42–45} As shown in Fig. 8, IHC analysis showed E-cadherin expression in the IUA group (1.188 ± 0.0473) was significantly decreased compared with that in the sham group (1.665 ± 0.1966). Whereas TC-Exo treatment significantly enhanced E-cadherin expression (1.507 ± 0.0427) (ANOVA, all P s < 0.05), indicating that TC-derived Exo can promote endometrial epithelium repair, which is in agreement with our previous study as well.⁷

Interestingly, no significant differences were observed for N-cadherin expression among three groups (sham: 1.466 ± 0.1918 ; IUA: 1.406 ± 0.1045 ; IUA-Exo: 1.408 ± 0.0985). This can be attributed to a prevalent expression of N-cadherin in non-epithelial tissues, including different types of cells, such as neural cells, endothelial cells, stromal cells, osteoblasts, and so on.^{46,47} Affections from TC-derived Exo might be overlapped and therefore cannot be significant reflected in non-epithelial tissues.

Discussion

The occurrence of IUAs has increased dramatically due to more frequent intrauterine interventions nowadays. The fundamental pathology of IUAs is endometrial fibrosis/scarring in response to various traumatic and inflammatory intrauterine alterations¹. Basically, re-epithelialization of ESCs by means of MET will periodically regenerate the endometrium after regular menstruation.¹² However, failure of such MET process will potentially cause endometrial defect, followed with initiation of ESCs being transformed into fibroblasts and myofibroblasts, excessive deposition and reorganization of ECM, finally leading to endometrial fibrosis or IUAs.^{10,11} A recent systematic review reported that among women with various types of miscarriage, the incidence of IUAs ranges from 6% to 30%.⁴⁸ Currently, fertility-sparing hysteroscopic adhesiolysis is the mainstream recommendation for treatment of IUAs, with ancillary various physical barriers and hormone therapy.^{49,50} Emerging new options include hyaluronic acid gel,⁵¹ improved hormone therapy,⁵² and platelet-rich plasma perfusion.⁵³ However, faced with adhesion recurrence rate being as high

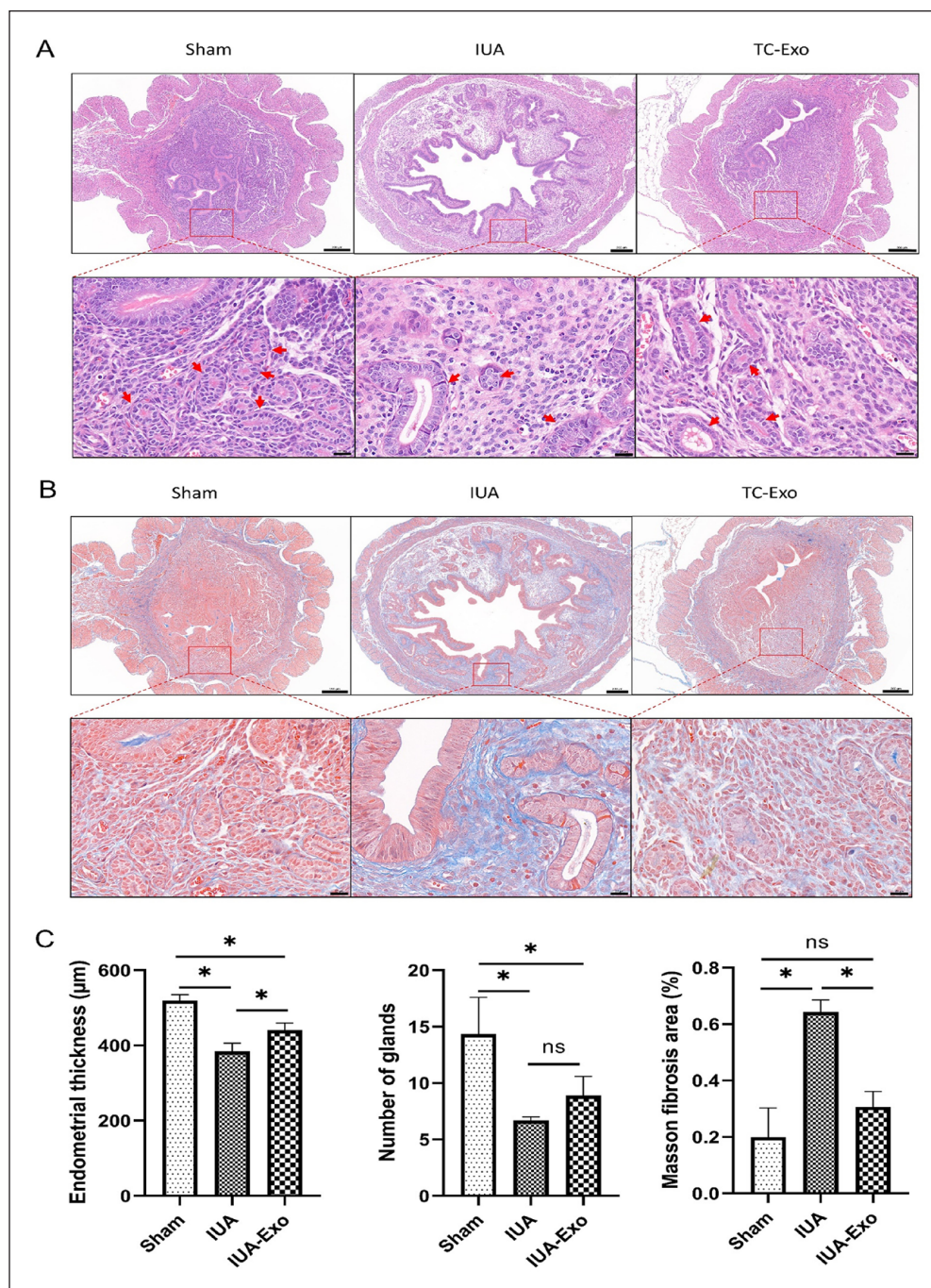


Figure 7. Morphometric analyses of endometrial thicknesses, number of endometrial glands, and fibrotic areas in IUA mouse model after TC-derived Exo treatment. Scale bar (from upper to lower enlarged images): 200, 20 μ m, respectively. (A) HE staining to observe endometrial thicknesses and glands (arrow). (B) Masson trichrome staining of endometrium, with blue-stained collagen fibers and red-stained mucosa, submucosa, muscles, and blood vessels. (C) Statistical analysis of endometrial thicknesses, number of endometrial glands, and fibrotic areas in each group. * $P < 0.05$, by ANOVA with Tukey's post hoc test, whereas ns indicates non-significant. IUA: intrauterine adhesion; TC: telocyte; HE: hematoxylin–eosin; ANOVA: analysis of variance.

as 62.5%,⁵⁴ and pregnancy and live birth rates being 66.1% and 64.0%,⁵⁵ these unsatisfied outcomes were main obstacles ahead of current treatment opinions. More recently, cell therapy demonstrates tremendous prospects for clinical application in treatment of IUAs. SC or SC-derived Exo

therapy, received extensive investigations both in lab and pre-clinic stage.^{56,57} Such as umbilical cord-derived mesenchymal stromal cells, which have been proved to be a safe and effective therapeutic approach for recurrent IUAs after adhesiolysis surgery.⁵⁸ In this study, for the first time, we

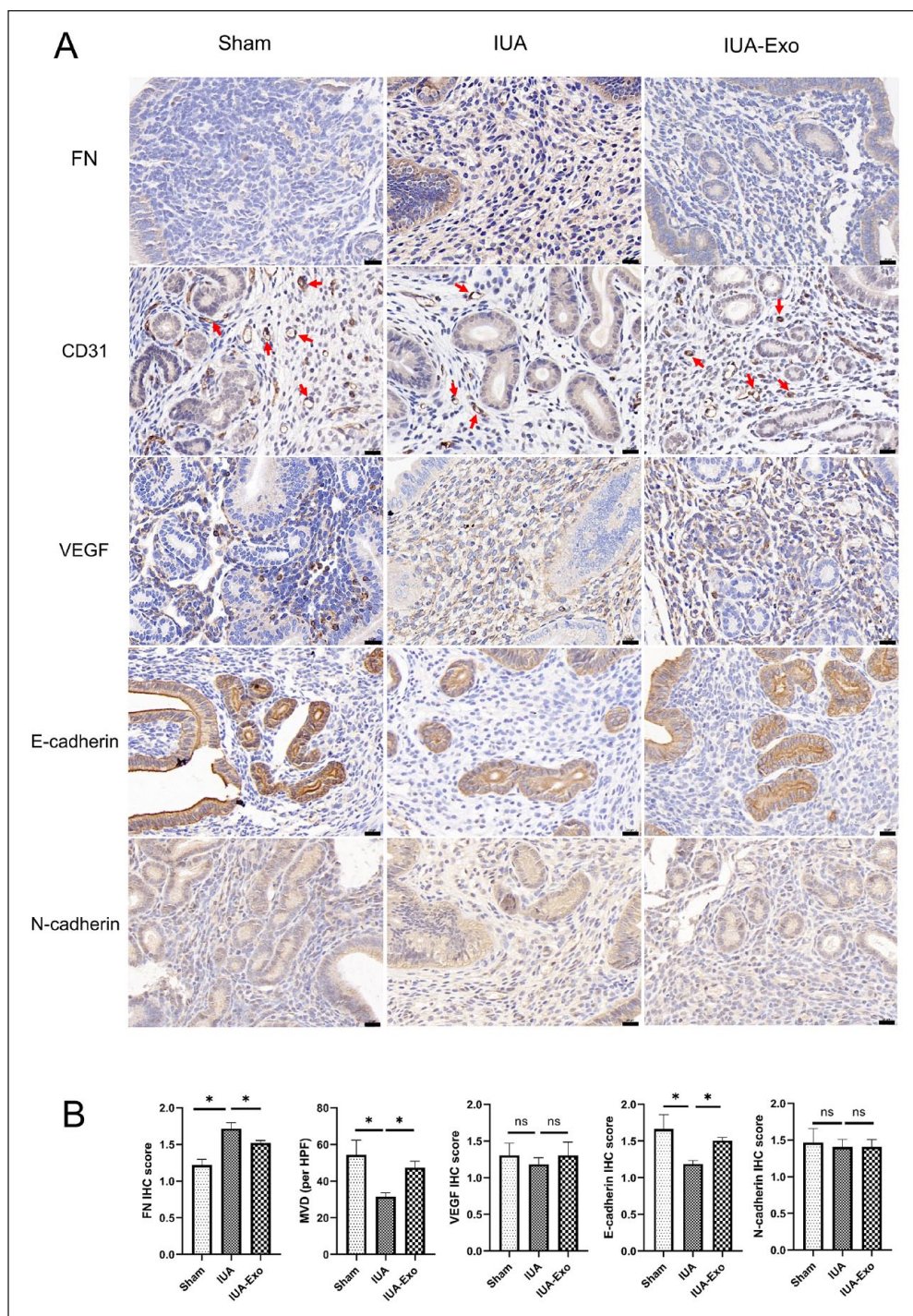


Figure 8. IHC of FN, CD31, VEGF, E-cadherin, and N-cadherin in uterine tissues from IUA mouse model. (A) IHC of FN, CD31, VEGF, E-cadherin, and N-cadherin in endometrial tissues. Arrow: CD31-positive endothelial cells. Scale bar = 20 μ m. (B) Semi-quantitative analysis of FN, MVD, VEGF, E-cadherin, and N-cadherin in each group. * $P < 0.05$, by ANOVA with Tukey's post hoc test, whereas ns indicates non-significant. IHC: immunohistochemistry; FN: fibronectin; VEGF: vascular endothelial growth factor.

reported that TC-derived Exo demonstrated exciting results to reverse fibrosis and enhance regeneration and repair both in cellular and IUA models.

TCs are newly found interstitial cells that have extremely long cellular prolongations known as Tps with alternating thin

(podomers) and thick segments (podoms). Tps was the key feature that distinguished TCs from any other cell and considered to be the ultrastructural hallmark.⁵⁹ Although TCs have no definite immunophenotypic characteristics, several reports claim that they have the ability to bind different antibodies.

However, according to the literature, it was considered that the double-positive immunostaining with CD34/PDGFR α and CD34/vimentin may be appropriate when referring to these cells.^{13,59–61} And in this study, the particular morphological characteristics and the double-positive immunostaining with CD34/vimentin were used to refer to TCs as earlier.^{7,20,21} TCs form a complex 3D network within interstitial tissues, with intercellular junctions between its long Tps and various adjacent cells, thus influencing their activities under different pathophysiological conditions.¹³ Apart from its 3D structural junctions in interstitial apartment, TCs also release rich amount of paracrine signaling substances, such as extracellular vesicles to regulate nearby cells.^{15,62} TCs play key roles in maintaining structural integrity of SC niches within intestinal mucosa crypts, providing different concentrations of Wnt ligands and Wnt inhibitors along the length of intestinal crypts. These signals were essential for nursing, self-renewal, differentiation of resident SC niche, and maintaining SC-mediated intestinal mucosal regeneration and repair.^{18,19} TC-driven Exo reduced cardiac fibrosis, improved heart function, increased angiogenesis in rats with myocardial infarction,¹⁷ and had been shown to benefit acute lung injury.⁶³ TCs have been found in female reproductive system as well, including vagina, uterus, uterine tube, ovary, and placenta.^{40,64} After TC loss and ensuing microenvironmental deregulation, premature ovarian failure may develop.⁶⁵ The lack of TC is related to the occurrence of leiomyomas, and Aleksandrovych et al.⁶⁶ provided immunohistochemical evidence of a diminished count of uterine TCs in leiomyomas. Placental TCs were located in the chorionic villi next to fetal blood vessels and myofibroblasts, and if TCs lost, the affected patients might be at a higher risk of developing preeclampsia.⁶⁷ TCs may be considered as the possible pathogenesis of endometriosis.⁶⁸ Loss or damage of TCs is closely related to fibrotic diseases in many other systems or organs, such as systemic sclerosis, ulcerative colitis, Crohn's disease, and liver fibrosis.^{16,69–73} Meanwhile, transplantation of TCs contributed to alleviation of fibrosis through reduction of ECM in disease-affected animal models.^{74,75}

In this study, TGF- β 1, a classic pro-fibrogenesis factor, at a concentration of 15 ng/ml was administrated to ESCs for 48 h to successfully develop fibrotic or IUA cell model, as identified by elevation of fibrotic markers (COL1A1, FN, and α -SMA). All of which were involved in cellular or tissue fibrogenesis.^{76,77}

Then, the fibrotic ESCs received TC-derived Exo treatment to observe reversal of fibrosis after such effectiveness was confirmed in TCM. The results showed that VEGF was significantly elevated with inhibited fibrotic markers, indicating salvage or reversal of fibrosis phenotype by TCs (either TCM or TC-derived Exo). Interestingly, the total secretion of VEGF in control ESCs was higher than the blank (culture medium for 48 h), but in the cells, the VEGF in control ESCs was lower than the blank (at 48 h). The reason for this difference may be that VEGF production was enhanced when initially exposed to TGF- β 1. Similar results were

reported before.^{78–80} But with the progression of fibrosis, VEGF secretion decreased in TGF- β 1 treated ESCs. Many factors can affect the expression of VEGF. In contrast to the cell model, there was no statistical difference in the level of VEGF expression in the animal model. This may be due to the more connections and interactions between different cell types in the uterus. Previously, our group reported TCM can induce elevation of E-cadherin and decreased N-cadherin in ESCs via Wnt/ β -catenin signaling pathway, subsequently enhancing decidualization and MET process in cultured ESCs.⁷ As we know, MET serves as one of the mechanisms of endometrial re-epithelialization after natural or artificial decidualization, which was the opposite direction against fibrosis process.¹² Currently, E-cadherin was elevated in IUA tissues after TC-derived Exo treatment. Therefore, combined with previous results,⁷ we speculate that the ability of TCs to reverse fibrosis may be achieved through the MET process. Similar result was observed in rat model of renal fibrosis, in which TC transplantation inhibited EMT (the opposite process of MET) to attenuate renal fibrosis.⁷⁵

Further pathway study showed that, after being administrated with ETC-159 and XAV939, which function to conditionally deplete Wnt ligands product within TCs and block Wnt/ β -catenin pathway within ESCs, TC-derived Exo lost its salvage effect on fibrosis. Interestingly, by means of bioinformatics analysis in a more recent study, Wnt signaling pathway was suggested to be involved in TCs mediated treatment of IUAs.⁸¹ Therefore, combined with previous pathway mechanisms,^{7,18,19,81} this study further confirms the participation of Wnt ligands and Wnt/ β -catenin pathway in the observed reversal effect on fibrotic ESCs. As we know, Wnt signaling is crucial for maintenance of stemness properties of SC, tissue homeostasis, and tissue development, especially for self-renewal of colon SC and endometrial mesenchymal stem-like cells.^{82–84} Besides, Wnt signaling pathway regulates tissue fibrosis, renewal, and regeneration in various tissues, including endometrium, lungs, kidney, and heart.^{85–87} Our work is in agreement with previous studies noting intestinal subepithelial Foxl1 and GLI1 positive TCs being an important non-epithelial source of Wnt ligands that supports stemness within intestinal crypts,^{18,19} uterine TCs were also proved to be an important source of Wnts that supports endometrium regeneration and fibrosis-resistant.

In vitro results were further verified by *in vivo* observations of IUA mouse model received TC-Exo treatment. Morphometric analyses showed obvious endometrium regeneration with enhanced angiogenesis and decreased fibrosis after TC-Exo treatment, as evidenced by the improved number of glands, significantly increased endometrial thickness, MVD, and VEGF, decreased fibrosis areas, and FN expression within endometrium. Therefore, TC-derived Exo played an important role in endometrium regeneration and reversal of endometrium fibrosis. Previously, exosomal delivery of multi-functional substances, containing mRNA, miRNA, and other non-coding RNA, DNA, proteins, and lipids, was proposed mechanisms

for mesenchymal SC-based therapy.^{88,89} Especially, bone marrow mesenchymal SC-derived Exo promoted repair of damaged endometrium.³⁷ More recently, TCs extracellular vesicles were reported to load with rich amounts of macromolecular signals, such as miRNA to adjacent cells. Such paracrine activity was supposed to enhance or alter the functional regulation of adjacent cells.^{14,15} High efficacy of TCs transplantation was observed in regeneration repair of cardiac and lung injury.^{90–92} Transplantation of cardiac TCs Exo, which was loaded with abundant miRNA-21-5P in rat model of myocardial infarct, can effectively increase MVD in infarcted and border zones, reduce infarction and fibrosis size, and finally improve myocardial function.⁹³ In calcific aortic valve disease (CAVD), by inhibiting Wnt/ β -catenin/Runx2 axis, TC-derived extracellular vesicles carrying miRNA-30b can reduce valve calcification and valve interstitial cells apoptosis.⁶⁰ Meanwhile, by transferring nutrients with TC-derived mediators and Exo, intraperitoneal administration of TCs not only showed significantly reduced pulmonary inflammation and edema but also facilitated proliferation and differentiation of airway epithelium in a rat model of LPS-induced lung injury.⁶³ Here, for the first time, we report that, by means of exosomal delivery of Wnt ligands, TC-derived Exo could inhibit fibrosis and support regeneration repair of endometrium.

Conclusion

In conclusion, our results confirmed that TC-derived Exo provided an important source of Wnts that inhibit fibrosis in fibrotic ESCs model and promote regeneration repair by relieving fibrosis and enhancing angiogenesis in the IUA mouse model. This study provided new evidence for therapeutic potential of TCs in fibrosis of endometrium, trauma, tissue engineering, or congenital-related uterine diseases.

Acknowledgments

The authors thank the experimental platform provided by the Institute of Blood and Marrow Transplantation of Soochow University.

Author Contributions

Conceptualization, T-QC and X-JY; methodology, T-QC, X-JW, and S-HZ; software, T-QC and X-JW; validation, T-QC and X-JY; formal analysis, T-QC, X-JY, and S-HZ; investigation, T-QC, H-YL, and X-JY; resources, X-JY; data curation, T-QC; writing—original draft preparation, T-QC and X-JY; writing—review and editing, H-YL, S-HZ, and X-JY; visualization, T-QC; supervision, H-YL, S-HZ, and X-JY; project administration, X-JY; funding acquisition, X-JY. All authors have read and agreed to the published version of the manuscript.

Ethical Approval

The research procedures involving animal were approved by the Ethics Committee of Soochow University (ECSU2019000163).

Statement of Human and Animal Rights

All of the experimental procedures used in this study were conducted in accordance with the Institutional Animal Care Guidelines of Soochow University. The animal welfare system was strictly followed during the research, and all efforts were made to reduce the suffering of the animals.

Statement of Informed Consent

There are no human subjects in this article, and informed consent is not applicable.

Declaration of Conflicting Interests

The author(s) declared no potential conflicts of interest with respect to the research, authorship, and/or publication of this article.

Funding

The author(s) disclosed receipt of the following financial support for the research, authorship, and/or publication of this article: This work was supported by the National Natural Science Foundation of China (grant number: 81971335).

ORCID iD

Xiao-Jun Yang  <https://orcid.org/0000-0001-5143-3357>

References

1. Yu D, Wong YM, Cheong Y, Xia E, Li TC. Asherman syndrome—one century later. *Fertil Steril*. 2008;89(4):759–79.
2. Kelleher AM, Milano-Foster J, Behura SK, Spencer TE. Uterine glands coordinate on-time embryo implantation and impact endometrial decidualization for pregnancy success. *Nat Commun*. 2018;9(1):2435.
3. Healy MW, Schexnayder B, Connell MT, Terry N, DeCherney AH, Csokmay JM, Yauger BJ, Hill MJ. Intrauterine adhesion prevention after hysteroscopy: a systematic review and meta-analysis. *Am J Obstet Gynecol*. 2016;215(3):267–75.e7.
4. Owusu-Akyaw A, Krishnamoorthy K, Goldsmith LT, Morelli SS. The role of mesenchymal–epithelial transition in endometrial function. *Hum Reprod Update*. 2018;25(1):114–33.
5. Deans R, Abbott J. Review of intrauterine adhesions. *J Minim Invasive Gynecol*. 2010;17(5):555–69.
6. Makieva S, Giacomini E, Ottolina J, Sanchez AM, Papaleo E, Vigano P. Inside the endometrial cell signaling subway: mind the Gap(s). *Int J Mol Sci*. 2018;19(9):2477.
7. Zhang FL, Huang YL, Zhou XY, Tang XL, Yang XJ. Telocytes enhanced in vitro decidualization and mesenchymal-epithelial transition in endometrial stromal cells via Wnt/beta-catenin signaling pathway. *Am J Transl Res*. 2020;12(8):4384–96.
8. Mohamed OA, Jonnaert M, Lebel-Dumais CL, Kuroda K, Clarke HJ, Dufort D. Uterine Wnt/beta-catenin signaling is required for implantation. *Proc Natl Acad Sci U S A*. 2005;102(24):8579–84.
9. Jeong JW, Lee HS, Franco HL, Broaddus RR, Taketo MM, Tsai SY, Lydon JP, DeMayo FJ. Beta-catenin mediates glandular formation and dysregulation of beta-catenin induces hyperplasia formation in the murine uterus. *Oncogene*. 2009;28(1):31–40.

10. Chen X, Liu J, He B, Li Y, Liu S, Wu B, Wang S, Zhang S, Xu X, Wang J. Vascular endothelial growth factor (VEGF) regulation by hypoxia inducible factor-1 alpha (HIF1A) starts and peaks during endometrial breakdown, not repair, in a mouse menstrual-like model. *Hum Reprod.* 2015;30(9):2160–70.
11. March CM. Asherman's syndrome. *Semin Reprod Med.* 2011;29(2):83–94.
12. Patterson AL, Zhang L, Arango NA, Teixeira J, Pru JK. Mesenchymal-to-epithelial transition contributes to endometrial regeneration following natural and artificial decidualization. *Stem Cells Dev.* 2013;22(6):964–74.
13. Vannucchi MG. The telocytes: ten years after their introduction in the scientific literature. An update on their morphology, distribution, and potential roles in the gut. *Int J Mol Sci.* 2020;21(12):4478.
14. Cretoiu D, Xu J, Xiao J, Cretoiu SM. Telocytes and their extracellular vesicles-evidence and hypotheses. *Int J Mol Sci.* 2016;17(8):1322.
15. Fertig ET, Gherghiceanu M, Popescu LM. Extracellular vesicles release by cardiac telocytes: electron microscopy and electron tomography. *J Cell Mol Med.* 2014;18(10):1938–43.
16. Wei XJ, Chen TQ, Yang XJ. Telocytes in fibrosis diseases: from current findings to future clinical perspectives. *Cell Transplant.* 2022;31:9636897221105252.
17. Yang J, Li Y, Xue F, Liu W, Zhang S. Exosomes derived from cardiac telocytes exert positive effects on endothelial cells. *Am J Transl Res.* 2017;9(12):5375–87.
18. Shoshkes-Carmel M, Wang YJ, Wangenstein KJ, Toth B, Kondo A, Massasa EE, Itzkovitz S, Kaestner KH. Subepithelial telocytes are an important source of Wnts that supports intestinal crypts. *Nature.* 2018;557(7704):242–46.
19. Degirmenci B, Valenta T, Dimitrova S, Hausmann G, Basler K. GLI1-expressing mesenchymal cells form the essential Wnt-secreting niche for colon stem cells. *Nature.* 2018;558(7710):449–53.
20. XLT. Telocytes enhanced the proliferation, adhesion and motility of endometrial stromal cells as mediated by the ERK pathway in vitro. *Am J Transl Res.* 2019;11(2):572–85.
21. Huang YL, Zhang FL, Tang XL, Yang XJ. Telocytes enhances M1 differentiation and phagocytosis while inhibits mitochondria-mediated apoptosis via activation of NF-kappaB in macrophages. *Cell Transplant.* 2021;30:9636897211002762.
22. Jiang XJ, Cretoiu D, Shen ZJ, Yang XJ. An in vitro investigation of telocytes-educated macrophages: morphology, heterocellular junctions, apoptosis and invasion analysis. *J Transl Med.* 2018;16(1):85.
23. Mehdiani A, Maier A, Pinto A, Barth M, Akhyari P, Lichtenberg A. An innovative method for exosome quantification and size measurement. *J Vis Exp.* 2015;95:50974.
24. Helwa I, Cai JW, Drewry MD, Zimmerman A, Dinkins MB, Khaled ML, Seremwe M, Dismuke WM, Bieberich E, Stamer WD, Hamrick MW, et al. A comparative study of serum exosome isolation using differential ultracentrifugation and three commercial reagents. *PLoS ONE.* 2017;12(1):e0170628.
25. Regente M, Corti-Monzon G, Maldonado AM, Pinedo M, Jorin J, de la Canal L. Vesicular fractions of sunflower apoplast fluids are associated with potential exosome marker proteins. *FEBS Lett.* 2009;583(20):3363–66.
26. Jung MK, Mun JY. Sample Preparation and imaging of exosomes by transmission electron microscopy. *J Vis Exp.* 2018(131):56482.
27. Tschuschke M, Kocherova I, Bryja A, Mozdziak P, Angelova Volponi A, Janowicz K, Sibiak R, Piotrowska-Kempisty H, Iżycki D, Bukowska D. Inclusion biogenesis, methods of isolation and clinical application of human cellular exosomes. *J Clin Med.* 2020;9(2):436.
28. Villarroya-Beltri C, Baixauli F, Mittelbrunn M, Fernández-Delgado I, Torralba D, Moreno-Gonzalo O, Baldanta S, Enrich C, Guerra S, Sánchez-Madrid F. ISGylation controls exosome secretion by promoting lysosomal degradation of MVB proteins. *Nat Commun.* 2016;7(1):13588.
29. Popovici RM, Irwin JC, Giaccia AJ, Giudice LC. Hypoxia and cAMP stimulate vascular endothelial growth factor (VEGF) in human endometrial stromal cells: potential relevance to menstruation and endometrial regeneration. *J Clin Endocrinol Metab.* 1999;84(6):2245–48.
30. Madan B, Ke Z, Harmston N, Ho SY, Frois AO, Alam J, Jeyaraj DA, Pendharkar V, Ghosh K, Virshup IH, Manoharan V, et al. Wnt addiction of genetically defined cancers reversed by PORCN inhibition. *Oncogene.* 2016;35(17):2197–2207.
31. Barrott JJ, Cash GM, Smith AP, Barrow JR, Murtaugh LC. Deletion of mouse Porcn blocks Wnt ligand secretion and reveals an ectodermal etiology of human focal dermal hypoplasia/Goltz syndrome. *Proc Natl Acad Sci U S A.* 2011;108(31):12752–57.
32. Sepramaniam S, Chew XH, Ngeow KC, Lee MA. ETC159, a porcupine inhibitor, exhibits synergism with PI3K inhibitors in 3-dimensional cell culture. *Cancer Res.* 2018;78(13):2939.
33. Tian XH, Hou WJ, Fang Y, Fan J, Tong H, Bai SL, Chen Q, Xu H, Li Y. XAV939, a tankyrase 1 inhibitor, promotes cell apoptosis in neuroblastoma cell lines by inhibiting Wnt/beta-catenin signaling pathway. *J Exp Clin Cancer Res.* 2013;32:100.
34. Huang SM, Mishina YM, Liu S, Cheung A, Stegmeier F, Michaud GA, Charlat O, Willellette E, Zhang Y, Wiessner S, Hild M, et al. Tankyrase inhibition stabilizes axin and antagonizes Wnt signalling. *Nature.* 2009;461(7264):614–20.
35. Zhao G, Li R, Cao Y, Song M, Jiang P, Wu Q, Zhou Z, Zhu H, Wang H, Dai C, Liu D, et al. DeltaNp63alpha-induced DUSP4/GSK3beta/SNAI1 pathway in epithelial cells drives endometrial fibrosis. *Cell Death Dis.* 2020;11(6):449.
36. Li J, Du S, Sheng X, Liu J, Cen B, Huang F, He Y. MicroRNA-29b inhibits endometrial fibrosis by regulating the Sp1-TGF-beta1/Smad-CTGF axis in a rat model. *Reprod Sci.* 2016;23(3):386–94.
37. Yao Y, Chen R, Wang G, Zhang Y, Liu F. Exosomes derived from mesenchymal stem cells reverse EMT via TGF-beta1/Smad pathway and promote repair of damaged endometrium. *Stem Cell Res Ther.* 2019;10(1):225.
38. Varghese F, Bukhari AB, Malhotra R, De A. IHC Profiler: an open source plugin for the quantitative evaluation and automated scoring of immunohistochemistry images of human tissue samples. *PLoS ONE.* 2014;9(5):e96801.
39. Weidner N. Intratumor microvessel density as a prognostic factor in cancer. *Am J Pathol.* 1995;147(1):9–19.
40. Roatesi I, Radu BM, Cretoiu D, Cretoiu SM. Uterine telocytes: a review of current knowledge. *Biol Reprod.* 2015;93(1):10.

41. Halper J. Basic components of connective tissues and extracellular matrix: fibronectin, fibrinogen, laminin, elastin, fibrillins, fibulins, matrilins, tenascins and thrombospondins. *Adv Exp Med Biol.* 2021;1348:105–26.
42. van Roy F, Berx G. The cell-cell adhesion molecule E-cadherin. *Cell Mol Life Sci.* 2008;65(23):3756–88.
43. Theys J, Jutten B, Habets R, Paesmans K, Groot AJ, Lambin P, Wouters BG, Lammering G, Vooijs M. E-Cadherin loss associated with EMT promotes radioresistance in human tumor cells. *Radiother Oncol.* 2011;99(3):392–97.
44. Loh CY, Chai JY, Tang TF, Wong WF, Sethi G, Shanmugam MK, Chong PP, Looi CY. The E-cadherin and N-cadherin switch in epithelial-to-mesenchymal transition: signaling, therapeutic implications, and challenges. *Cells.* 2019;8(10):1118.
45. Han L, Luo H, Huang W, Zhang J, Wu D, Wang J, Pi J, Liu C, Qu X, Liu H. Modulation of the EMT/MET Process by E-cadherin in airway epithelia stress injury. *Biomolecules.* 2021;11(5):669.
46. van Roy F. Beyond E-cadherin: roles of other cadherin superfamily members in cancer. *Nat Rev Cancer.* 2014;14(2):121–34.
47. Mrozik KM, Blaschuk OW, Cheong CM, Zannettino ACW, Vandyke K. N-cadherin in cancer metastasis, its emerging role in haematological malignancies and potential as a therapeutic target in cancer. *BMC Cancer.* 2018;18(1):939.
48. Salazar CA, Isaacson K, Morris S. A comprehensive review of Asherman's syndrome: causes, symptoms and treatment options. *Curr Opin Obstet Gynecol.* 2017;29(4):249–56.
49. Yang JH, Chen CD, Chen SU, Yang YS, Chen MJ. The influence of the location and extent of intrauterine adhesions on recurrence after hysteroscopic adhesiolysis. *BJOG.* 2016;123(4):618–23.
50. Surgery AEG. AAGL practice report: practice guidelines on intrauterine adhesions developed in collaboration with the European Society of Gynaecological Endoscopy (ESGE). *J Minim Invasive Gynecol.* 2017;24(5):695–705.
51. Acunzo G, Guida M, Pellicano M, Tommaselli GA, Di Spiezio Sardo A, Bifulco G, Cirillo D, Taylor A, Nappi C. Effectiveness of auto-cross-linked hyaluronic acid gel in the prevention of intrauterine adhesions after hysteroscopic adhesiolysis: a prospective, randomized, controlled study. *Hum Reprod.* 2003;18(9):1918–21.
52. Zhang SS, Xia WT, Xu J, Xu HL, Lu CT, Zhao YZ, Wu XQ. Three-dimensional structure micelles of heparin-poloxamer improve the therapeutic effect of 17 β -estradiol on endometrial regeneration for intrauterine adhesions in a rat model. *Int J Nanomedicine.* 2017;12:5643–57.
53. Albazee E, Al-Rshoud F, Almahmoud L, Al Omari B, Alnifise M, Baradwan S, Abu-Zaid A. Platelet-rich plasma for the management of intrauterine adhesions: a systematic review and meta-analysis of randomized controlled trials. *J Gynecol Obstet Hum Reprod.* 2022;51(2):102276.
54. Chen Y, Liu L, Luo Y, Chen M, Huan Y, Fang R. Prevalence and impact of chronic endometritis in patients with intrauterine adhesions: a prospective cohort study. *J Minim Invasive Gynecol.* 2017;24(1):74–79.
55. Xiao S, Wan Y, Xue M, Zeng X, Xiao F, Xu D, Yang X, Zhang P, Sheng W, Xu J, Zhou S. Etiology, treatment, and reproductive prognosis of women with moderate-to-severe intrauterine adhesions. *Int J Gynaecol Obstet.* 2014;125(2):121–24.
56. Xin L, Lin X, Pan Y, Zheng X, Shi L, Zhang Y, Ma L, Gao C, Zhang S. A collagen scaffold loaded with human umbilical cord-derived mesenchymal stem cells facilitates endometrial regeneration and restores fertility. *Acta Biomater.* 2019;92:160–71.
57. Song YT, Liu PC, Tan J, Zou CY, Li QJ, Li-Ling J, Xie HQ. Stem cell-based therapy for ameliorating intrauterine adhesion and endometrium injury. *Stem Cell Res Ther.* 2021;12(1):556.
58. Cao Y, Sun H, Zhu H, Zhu X, Tang X, Yan G, Wang J, Bai D, Wang J, Wang L, Zhou Q, et al. Allogeneic cell therapy using umbilical cord MSCs on collagen scaffolds for patients with recurrent uterine adhesion: a phase I clinical trial. *Stem Cell Res Ther.* 2018;9(1):192.
59. Cretoi SM, Popescu LM. Telocytes revisited. *Biomol Concepts.* 2014;5(5):353–69.
60. Yang R, Tang Y, Chen X, Yang Y. Telocytes-derived extracellular vesicles alleviate aortic valve calcification by carrying miR-30b. *ESC Heart Fail.* 2021;8(5):3935–46.
61. Chi C, Jiang XJ, Su L, Shen ZJ, Yang XJ. In vitro morphology, viability and cytokine secretion of uterine telocyte-activated mouse peritoneal macrophages. *J Cell Mol Med.* 2015;19(12):2741–50.
62. Fausone-Pellegrini MS, Gherghiceanu M. Telocyte's contacts. *Semin Cell Dev Biol.* 2016;55:3–8.
63. Tang L, Song D, Qi R, Zhu B, Wang X. Roles of pulmonary telocytes in airway epithelia to benefit experimental acute lung injury through production of telocyte-driven mediators and exosomes. *Cell Biol Toxicol.* 2023;39(2):451–65.
64. Janas P, Kucybala I, Radon-Pokracka M, Huras H. Telocytes in the female reproductive system: an overview of up-to-date knowledge. *Adv Clin Exp Med.* 2018;27(4):559–65.
65. Liu T, Wang S, Li Q, Huang Y, Chen C, Zheng J. Telocytes as potential targets in a cyclophosphamide-induced animal model of premature ovarian failure. *Mol Med Rep.* 2016;14(3):2415–22.
66. Aleksandrovykh V, Białas M, Pasternak A, Bereza T, Sajewicz M, Walocha J, Gil K. Identification of uterine telocytes and their architecture in leiomyoma. *Folia Med Cracov.* 2018;58(3):89–102.
67. Abu-Dief EE, Elsayed HM, Atia EW, Abdel-Rahman M, Fawzy M. Modulation of telocytes in women with preeclampsia: a prospective comparative study. *J Microsc Ultrastruct.* 2021;9(4):158–63.
68. Xu T, Zhang H, Zhu Z. Telocytes and endometriosis. *Arch Gynecol Obstet.* 2023;307(1):39–49.
69. Yang XJ, Yang J, Liu Z, Yang G, Shen ZJ. Telocytes damage in endometriosis-affected rat oviduct and potential impact on fertility. *J Cell Mol Med.* 2015;19(2):452–62.
70. Milia AF, Ruffo M, Manetti M, Rosa I, Conte D, Fazi M, Messerini L, Ibba-Manneschi L. Telocytes in Crohn's disease. *J Cell Mol Med.* 2013;17(12):1525–36.
71. Manetti M, Rosa I, Messerini L, Ibba-Manneschi L. Telocytes are reduced during fibrotic remodelling of the colonic wall in ulcerative colitis. *J Cell Mol Med.* 2015;19(1):62–73.
72. Manetti M, Guiducci S, Ruffo M, Rosa I, Fausone-Pellegrini MS, Matucci-Cerinic M, Ibba-Manneschi L. Evidence for progressive reduction and loss of telocytes in the dermal cellular network of systemic sclerosis. *J Cell Mol Med.* 2013;17(4):482–96.

73. Fu S, Wang F, Cao Y, Huang Q, Xiao J, Yang C, Popescu LM. Telocytes in human liver fibrosis. *J Cell Mol Med*. 2015;19(3):676–83.
74. Zhao B, Liao Z, Chen S, Yuan Z, Yilin C, Lee KK, Qi X, Shen X, Zheng X, Quinn T, Cai D. Intramyocardial transplantation of cardiac telocytes decreases myocardial infarction and improves post-infarcted cardiac function in rats. *J Cell Mol Med*. 2014;18(5):780–89.
75. Zheng L, Li L, Qi G, Hu M, Hu C, Wang S, Li J, Zhang M, Zhang W, Zeng Y, Zhang Y, et al. Transplantation of Telocytes Attenuates Unilateral Ureter Obstruction-Induced Renal Fibrosis in Rats. *Cell Physiol Biochem*. 2018;46(5):2056–71.
76. Liu L, Chen G, Chen T, Shi W, Hu H, Song K, Huang R, Cai H, He Y. Si-SNHG5-FOXF2 inhibits TGF- β 1-induced fibrosis in human primary endometrial stromal cells by the Wnt/ β -catenin signalling pathway. *Stem Cell Res Ther*. 2020;11(1):479.
77. Li J, Cen B, Chen S, He Y. MicroRNA-29b inhibits TGF- β 1-induced fibrosis via regulation of the TGF- β 1/Smad pathway in primary human endometrial stromal cells. *Mol Med Rep*. 2016;13(5):4229–37.
78. Kariya T, Nishimura H, Mizuno M, Suzuki Y, Matsukawa Y, Sakata F, Maruyama S, Takei Y, Ito Y. TGF- β 1-VEGF-A pathway induces neoangiogenesis with peritoneal fibrosis in patients undergoing peritoneal dialysis. *Am J Physiol Renal Physiol*. 2018;314(2):F167–80.
79. Jeon SH, Chae BC, Kim HA, Seo GY, Seo DW, Chun GT, Kim NS, Yie SW, Byeon WH, Eom SH, Ha KS, et al. Mechanisms underlying TGF- β 1-induced expression of VEGF and Flk-1 in mouse macrophages and their implications for angiogenesis. *J Leukoc Biol*. 2007;81(2):557–66.
80. Kobayashi T, Liu X, Wen FQ, Fang Q, Abe S, Wang XQ, Hashimoto M, Shen L, Kawasaki S, Kim HJ, Kohyama T, et al. Smad3 mediates TGF- β 1 induction of VEGF production in lung fibroblasts. *Biochem Biophys Res Commun*. 2005;327(2):393–98.
81. Zhao C-z, Fu P, Peng W-y, Pan N, Peng Y, Zhao M, Xie W. The mechanism of Wnt pathway regulated by telocytes to promote the regeneration and repair of intrauterine adhesions. *Comput Math Methods Med*. 2022;2022:3809792.
82. Farin HF, Jordens I, Mosa MH, Basak O, Korving J, Tauriello DV, de Punder K, Angers S, Peters PJ, Maurice MM, Clevers H. Visualization of a short-range Wnt gradient in the intestinal stem-cell niche. *Nature*. 2016;530(7590):340–43.
83. Clevers H, Loh KM, Nusse R. Stem cell signaling. An integral program for tissue renewal and regeneration: Wnt signaling and stem cell control. *Science*. 2014;346(6205):1248012.
84. Cao M, Chan RWS, Cheng FHC, Li J, Li T, Pang RTK, Lee CL, Li RHW, Ng EHY, Chiu PCN, Yeung WSB. Myometrial cells stimulate self-renewal of endometrial mesenchymal stem-like cells through WNT5A/ β -catenin signaling. *Stem Cells*. 2019;37(11):1455–66.
85. Ozhan G, Weidinger G. Wnt/ β -catenin signaling in heart regeneration. *Cell Regen*. 2015;4(1):3.
86. Raslan AA, Yoon JK. WNT signaling in lung repair and regeneration. *Mol Cells*. 2020;43(9):774–83.
87. Cao J, Liu D, Zhao S, Yuan L, Huang Y, Ma J, Yang Z, Shi B, Wang L, Wei J. Estrogen attenuates TGF- β 1-induced EMT in intrauterine adhesion by activating Wnt/ β -catenin signaling pathway. *Braz J Med Biol Res*. 2020;53(8):e9794.
88. Kang K, Ma R, Cai W, Huang W, Paul C, Liang J, Wang Y, Zhao T, Kim HW, Xu M, Millard RW, et al. Exosomes secreted from CXCR4 overexpressing mesenchymal stem cells promote cardioprotection via Akt signaling pathway following myocardial infarction. *Stem Cells Int*. 2015;2015:659890.
89. Huang YC, Parolini O, Deng L. The potential role of microvesicles in mesenchymal stem cell-based therapy. *Stem Cells Dev*. 2013;22(6):841–44.
90. Bei Y, Zhou Q, Sun Q, Xiao J. Telocytes in cardiac regeneration and repair. *Semin Cell Dev Biol*. 2016;55:14–21.
91. Zhou Y, Yang Y, Liang T, Hu Y, Tang H, Song D, Fang H. The regulatory effect of microRNA-21a-3p on the promotion of telocyte angiogenesis mediated by PI3K (p110 α)/AKT/mTOR in LPS induced mice ARDS. *J Transl Med*. 2019;17(1):427.
92. Zhang D, Song D, Shi L, Sun X, Zheng Y, Zeng Y, Wang X. Mechanisms of interactions between lung-origin telocytes and mesenchymal stem cells to treat experimental acute lung injury. *Clin Transl Med*. 2020;10(8):e231.
93. Liao Z, Chen Y, Duan C, Zhu K, Huang R, Zhao H, Hintze M, Pu Q, Yuan Z, Lv L. Cardiac telocytes inhibit cardiac microvascular endothelial cell apoptosis through exosomal miRNA-21-5p-targeted cdipl silencing to improve angiogenesis following myocardial infarction. *Theranostics*. 2021;11(1):268–91.